Available online at www.sciencedirect.com
SCIENCE DIRECT®
C. R. Physique 4 (2003) 571–594
COMPTES RENDUS PHYSIQUE

Exotic nuclei/Les noyaux exotiques

On the production of superheavy elements

Peter Armbruster

Gesellschaft für Schwerionenfoschung mbH, Nuclear Physics II Division, Planckstraße 1, 64291 Darmstadt, Germany

Presented by Guy Laval

Abstract

Since the discovery of Deformed Superheavy Nuclei (1983–85) a bridge connects the island of SHE to known isotopes of lighter elements. What we know experimentally and theoretically on the nuclear structure of SHE is reported in a first section. The making of the elements, with an analysis of production cross sections, and the macroscopic limitation to $Z = 112 + \varepsilon$ is presented in a second section. The break-down of fusion cross sections in the 'Coulomb Falls' within a range of about 10 elements is introduced as the universal limiting phenomenon. How the nuclear structure of the collision partners modifies the on-set of this limitation is presented in Section 3. Reactions induced by deformed nuclei are pushed by side collisions to higher excitation energies (4n- and 5n-channels), whereas reactions driven by the cluster-like, closed-shell nuclei, $^{208}_{126}$Pb and $^{138}_{82}$Ba, are kept at low excitation energies (1n- and 2n-channels). The on-set of production limitation for deformed collision partners is moved to smaller effective fissilities $x = 0.68 \leqslant 0.72$, whereas for spherical clusters the on-set is delayed $x = 0.76 \geqslant 0.72$ and $x = 0.79 \geqslant 0.72$ for ^{138}Ba and ^{208}Pb, respectively. An outlook, what remains to be studied in the future, ends the article. ***To cite this article: P. Armbruster, C. R. Physique 4 (2003).***

Résumé

Sur la production des éléments super lourd. Depuis la découverte de noyaux super lourds déformés (1983–85) un « pont » relie l'îlot des noyaux super lourds (SHE) aux isotopes connus des éléments plus légers. Ce que nous savons, tant d'un point de vue expérimental que théorique, de la structure des SHE est présenté dans la première section. La synthèse de nouveaux éléments, l'analyse des sections efficaces de production ainsi que la limitation macroscopique de ces études à l'élément $Z = 112 + \varepsilon$ fait l'objet de la deuxième section. L'annulation des sections efficaces de fusion d'éléments chargés d'une dizaine de protons supplémentaire est introduite comme une conséquence générale de la répulsion Coulombienne (« Coulomb Falls »). La manière dont la structure des partenaires de la collision modifie cette limite Coulombienne est présentée dans la Section 3. Les réactions induites par des noyaux déformés conduisent à des noyaux plus excités (décroisant en émettant plus de neutrons (Canaux à 4n et 5n)) alors que celles mettant en jeu des noyaux avec des sous structure en agrégats et les noyaux à couches fermés, $^{208}_{126}$Pb et $^{138}_{82}$Ba conservent des excitations faibles (Canaux à 1n et 2n)). Le début de l'annulation de production de SHE par la fusion de noyaux déformés est abaissée à une plus petite fissilité $x = 0.68 \leqslant 0.72$, alors que pour des noyaux sphériques elle se retrouve accrue $x = 0.76 \geqslant 0.72$ pour le ^{138}Ba et $x = 0.79 \geqslant 0.72$ pour le ^{208}Pb. Un point sur les travaux qu'il reste à mener termine cette revue. ***Pour citer cet article : P. Armbruster, C. R. Physique 4 (2003).***

E-mail address: P.Armbruster@GSI.DE (P. Armbruster).

1631-0705/03/$ – see front matter
doi:10.1016/S1631-0705(03)00061-6

1. Changing the concepts of superheavy elements

1.1. An island behind the swamp (1966–1984)

Studies on fusion reactions and on Pb/Bi-based reactions were in the focus of SHIP experiments during the UNILAC-period (1976–1990) of GSI [1]. Using our recoil-separation technique, implantation into active detectors, and correlation analysis of decay-chains opened a new physical method for heavy element research. We checked the earlier Dubna-experiments [2] using ^{208}Pb- and ^{209}Bi-targets combined with beams of ^{50}Ti- and ^{54}Cr-beams. The 1n-channel in these reactions was discovered in 1980 via the production of ^{257}Rf with 10 nb in the reaction ^{50}Ti/^{208}Pb. This discovery opened for our group the passage towards ^{277}112, which finally was reached 16 years later with 0.5 pb by replacing ^{50}Ti by ^{70}Zn [3]. Six elements were discovered at GSI, repeatedly applying the 1n-channel reactions. The elements Bh (107), Hs (108), Mt (109), 110, 111, and 112 were synthesized with steadily decreasing cross sections in the complete fusion of ^{208}Pb and ^{209}Bi with the most n-rich stable e–e-isotopes of the elements $Z = 24$–30. On average, a factor 3.8 had to be paid reaching the next higher element on this long journey, passing the former swamp of instability. How did we manage to pass the obstacle?

Starting to play cautiously on the shores of the swamp we found our first element $Z = 107$ with ^{262}107, now bohrium in early 1981 [4]. O–O-isotopes were known to be specially stable against spontaneous fission decay. We took this argument and argued that the next try should go to an O–O-isotope of $Z = 109$, now meitnerium, replacing the ^{54}Cr-projectiles by ^{58}Fe. We discovered in 1982 the isotope ^{266}Mt detecting a single chain with one new correlated α-particle, preceding the known chain of ^{262}Bh [5,6].

I remember 1983 started as a year of open questions and discussions. ^{266}Mt$_{157}$ and ^{263}Sg$_{157}$, the last nuclei synthesized at LBL in 1974 [7], have the same number of neutrons. We had just added three protons to the heaviest nucleus known before we started our work. What are the orbitals for the 3 protons, which increase the height of the fission barrier in order to compensate the steady decrease of the barriers approaching higher atomic numbers? Is that possible at all? Is the impenetrable swamp of spontaneous fission of that time just a plausible explanation and welcome excuse to end heavy element synthesis at atomic number 106? The discussion on the nuclear structure of SHE was barred since 1966 by the idea of spherical nuclei, which should give the largest stabilization to a fission barrier at $Z = 114$ [8,9]. The separated island of spherical nuclei, a child of the shell-model, and the rapid break-down of stability against spontaneous fission-decay with increasing atomic number, a late child of the liquid drop-model, generated the swamp.

Nuclear structure of deformed nuclei known to stabilize nuclear ground states in large regions below ^{208}Pb was marginalized as of no importance for the heaviest elements. There was only a minor theoretical effort to understand the deformed nuclei in the swamp contrasting the very large number of papers on the spherical nuclei on the island. In 1974, A. Sobiczewski presented a 'Review on Recent Predictions' at the 27th Nobel Symposium in Physics, and A. Bohr in the discussion gave a comment [10]: "We have heard a great deal about the search of superheavy nuclei with a spherical shape? What about the possibility of SHE in other shapes stabilized by shell structure?"

An important paper of S. Cwiok, V.V. Paskhevich, F. Dudek, and W. Nazarevicz, appeared in 1983 [11] on deformed nuclei in the range 104–110. The authors replaced the Nilsson single particle potential formerly used by a Wood-Saxon potential and introduced the full 5 parameter (β_2–β_4)-deformation space to calculate shell corrections. They predicted high fission barriers and increased stability for deformed nuclei centered around ^{270}Hs, a finding against the rules of the time. At the end of the 1983, a careful investigation on the spontaneously fissioning isotopes of elements $Z = 104$ and $Z = 106$ was published by A.G. Demin, S.P. Tretyakova, V.K. Utyonkov, and I.V. Shirokovsky [12]. It was proposed that the sf-isotopes, formerly assigned to $Z = 106$, might be the α-decay daughters of Sg-isotopes, that is isotopes of $Z = 104$. The higher element $Z = 106$ should be more stable against spontaneous fission than $Z = 104$, another finding against the rules of the time. At GSI we detected the α–sf-correlations of ^{260}Sg/^{256}Rf only a few months later in January 1984 by establishing the α-decay of an e–e-isotope of $Z = 106$. These experiments seriously questioned the existence of the swamp of instability. The final proof of increasing stability against spontaneous fission for elements beyond Rf was given by the discovery of element 108 discovered 14 February 1984 [13]. In my lecture June 1984 at the 91th Fermi–School in honor of H. Bethe at Varenna, I elaborated from the unexpected finding of high fission barriers up to $Z = 109$ the possibility to reach elements ($Z = 110$–114) along a window of decay chains following N–$Z = 50 \pm 3$ [14]. These isotopes should decay by α-chains reaching well-known isotopes of the lighter elements Sg to No. It was in this corridor, in which the elements $Z = 110$ to $Z = 112$ were discovered more than 10 years later at GSI [3,15,16]. P. Möller, whom I met in Berkeley in spring 1984, immediately reacted on our discovery of Hs ($Z = 108$) and calculated with R. Nix in Los Alamos shell corrections for the isotopes $Z < 112$ and $N < 170$. An increase of sf-stability was confirmed including β_4-deformations of these isotopes [17]. A. Sobiczewski and S. Cwiok started, based on the 1983 S. Cwiok and V.V. Paskhevich paper [11], a careful study which established convincingly in an increased deformation-space including β_6-deformation, the island of deformed barrel-like ($\beta_4 < 0$) purely shell-stabilized nuclei centered at ^{270}Hs. At the end of 1984 I started to speak of 'deformed superheavies' in talks presenting the state of the field, and in 1986 A. Sobiczewski et

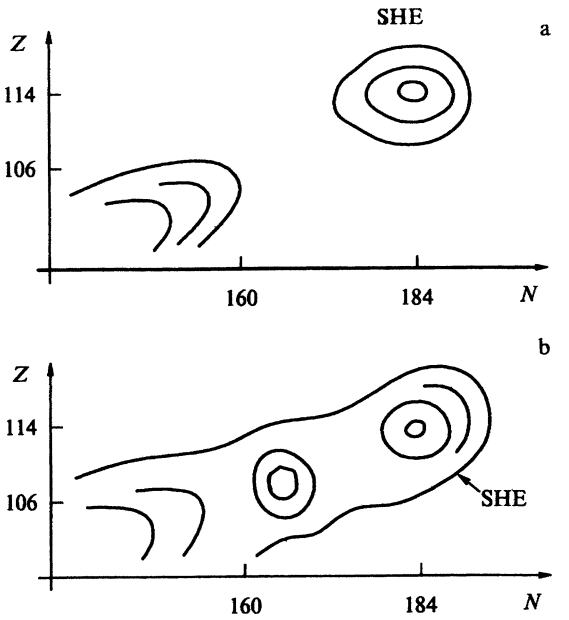

Fig. 1. Regions of relatively long-lived nuclei; as believed earlier a) and expected presently [19].

al. introduced in their following papers this term into the literature [18,19], Fig. 1. Since then there are two regions of purely shell-stabilized elements, deformed SHE centered at ^{270}Hs and spherical SHE for elements $Z = 114$–124, $N = 172$–184.

1983/1984, within less than a year in a common effort of experiment and theory, the picture of heavy element stability changed: the swamp of instability was drained and bridged by the deformed SHE.

2. SHE – born out of nuclear structure

2.1. Fission barriers, shell-corrections, and experimental masses

The microscopic corrections to the binding energy of heavy nuclei are of the same order as the smoothly varying liquid-drop barriers, which are chosen as a scaling reference. The ratio of shell corrections and the liquid-drop barriers are underlying the presentation of heavy nuclides shown in Fig. 2. The double-shell closures at ^{208}Pb and at $^{298}120_{178}$ are the centers of regions of spherical nuclei, which are separated by a wide region of deformed nuclei. Sub-shells at $^{252}_{152}$Fm, $^{270}_{162}$Hs, and $^{292}_{172}120$ are indicated. The outer contour lines of Fig. 2 correspond to half-lives of about 10^{-6} s and represent the detection limit of today's experiments. Numbers indicate different regions defined by different ratios of shell corrections to liquid-drop barriers. In region (1) the liquid-drop barrier has fallen below the zero-point energy ($B_f = 0.5$ MeV). Shell corrections dominate and give high and narrow fission barriers that protect against spontaneous fission decay. This is the region of SHE ($Z = 107$–124), where we find the deformed superheavy isotopes (D-SHE) and spherical (S-SHE) isotopes. The D-SHE extend from $^{260}Sg_{154}$ to $^{280}112_{168}$ and are centered around $^{270}Hs_{162}$. They are followed by the S-SHE extending to $^{308}124$ and being centered around $^{298}120$. All in all, we expect more than 300 isotopes, the ground states of which are protected against immediate spontaneous fission decay by a local microscopic correction to their binding energies, but only about 50 isotopes in the green region can be made by complete fusion. Going further down to the region (2), from Sg ($Z = 106$) to Fm ($Z = 100$) the shell correction energies become weaker, but the liquid-drop barriers start to increase. Here, spontaneous fission becomes a dominant decay mode at Rf ($Z = 104$). Region (3) shows shell correction energies and liquid-drop barriers of about equal height, starting with a ratio of 2 and ending with a ratio of 0.5 for these quantities. We find two subregions. First, at $N = 126$ there are strongly shell-stabilized spherical nuclei for elements above radium with barriers twice their liquid drop fission barriers. They are observed up to U, but are elusive beyond [20]. These nuclei are the best approximation to the spherical superheavy nuclei at $N = 172$–184, which are elusive as well. Second, between Es ($Z = 99$) and Pu ($Z = 94$) we find the well-studied region of deformed nuclei and fission isomers [21] characterized by the interplay of shell correction energies and the increasing liquid-drop barriers. In this region the most complex nuclear structure is expected. Region (4) is dominated by liquid drop barriers ($Z = 89$–93). Below the line of equal neutron binding energy and liquid drop barriers ($Z < 88$) in region (5), fission is observed at high excitation

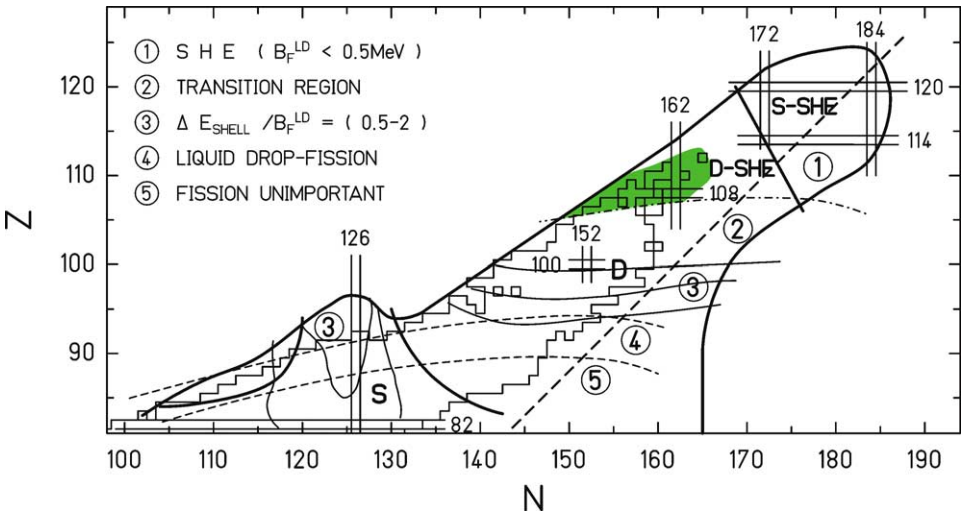

Fig. 2. The region of shell-stabilized nuclei may be divided in five sub-regions defined by the ratio of the height of the shell correction energies to the macroscopic fission barriers. Regions of spherical (S) and deformed (D) nuclei, shells and subshells between ^{208}Pb and ^{304}120 are indicated. $N-Z = 62$ is indicated by the hatched line, beyond which no compound nuclei can be synthesized by combinations of available collision partners. In the shaded region about 50 isotopes of D-SHE are found, which can be produced in complete fusion reactions and are presented in Fig. 17.

energies only, and is not important for the ground state decay and the properties of nuclei at low excitation energy. The spirit of Figs. 1 and 2 is the same. There is one world of atomic nuclei surrounded by the three instabilities: drip lines for protons and neutrons and binary break-up by spontaneous fission.

Superheavy nuclei decaying by ground-state to ground-state α-decays yield directly the binding energy difference between the parent and daughter nuclei. The α-decay of e–e-nuclei predominantly populates the ground state and the mass-excess of the parent nucleus is obtained by summing the measured α-decay energy and the known mass-excess of the daughter nucleus. Alpha-decay chains connect nuclei with the same $(N-Z)$-value and a chain of e–e-nuclei bridges a region of atomic numbers equal to twice the number of α-decay generations. The mass-excess values of the e–e-nuclei in the chain $(N-Z) = 48$ between $Z = 108$ and $Z = 102$ were measured in experiments at GSI using 1n- and 2n-reactions on ^{207,208}Pb targets [22–24].

The difference between the calculated mass-excesses of a structureless macroscopic nuclear model [25] and the measured values gives the shell-correction energies. In the spirit of the early paper of Swiatecki [26], which introduced the concept of microscopic corrections to nuclear binding energies, the shell correction energies of the heaviest nuclei were determined for the known e–e-isotopes of transuranic isotopes [14,27]. These are presented in Fig. 3(a), which is taken from a paper published 1989 together with Z. Patyk and A. Sobiczewski [28].

Neglecting the microscopic correction of the binding energy at the saddle point, the fission barrier height is obtained by summing the fission barrier calculated from a macroscopic model and the experimental ground-state shell-correction, Fig. 3(b). The negative shell corrections are strongest for $^{208}_{126}$Pb. They become weaker going to higher masses, and they reach values close to zero near $A = (224–228)$. Increasing A further, approaching the next shell at $^{270}_{162}$Hs they are steadily reinforced again and reach values of $-(5–6)$ MeV, Fig. 3(a). The fission barriers between U and Hs are high and stay in the range of (5 ± 0.5) MeV, Fig. 3(b). The decrease of the macroscopic fission barriers reaching values close to the zero-point vibrational energy of 0.5 MeV at Sg is compensated by the steadily increasing microscopic shell corrections of the ground-state binding energies.

The fact that these nuclei decay by α-emission shows that the fission barriers are high enough to protect the nuclei against immediate spontaneous fission. It is the internal structure that makes the ground-state shell corrections large. Locally restricted in the deformation space around the ground-state a hole in the potential energy surface appears, which is equivalent to raise a fission barrier stabilizing the nuclear system even in the case of macroscopic instability. The α-decay in the $N-Z = 48$ chain proves that fission barriers for e–e nuclei are high enough, at least up to $Z = 108$, to guarantee decay times of spontaneous fission that are longer than the α-decay half-lives, which are on the order of 10^{-3} s. ^{264}Hs has all characteristics required for a superheavy e–e isotope.

Moreover, the analysis of masses and half-lives in the chain $N-Z = 48$ gave not only fission barriers but also estimates of the curvature of the barriers [22]. Beyond $Z = 102$, the barrier curvature increases by a factor of 2 compared with isotopes of lighter actinides. Here, a decrease of the fission barrier by 1 MeV changes the spontaneous fission half-life by only 3–4 orders of magnitude, as compared to the 7 orders of magnitude found for the broad barriers of lighter elements. Fig. 4 shows the calculated

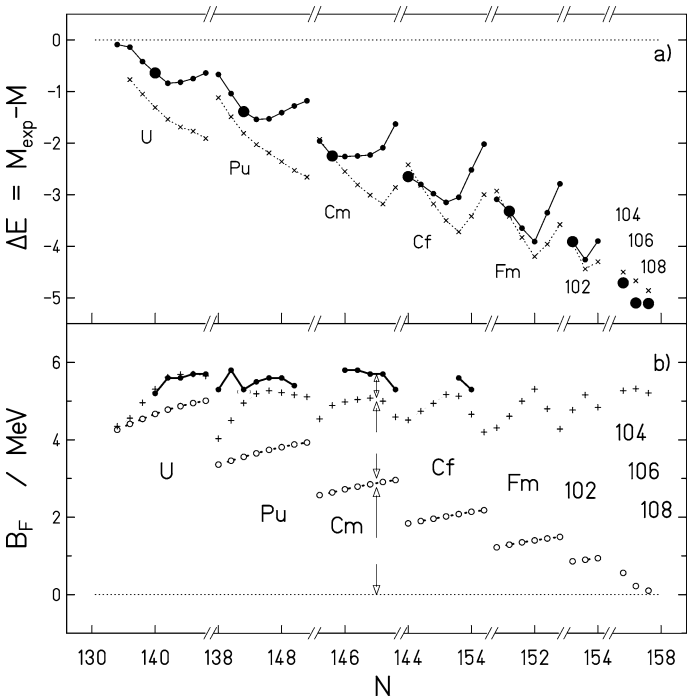

Fig. 3. For the known e–e isotopes of elements U to Hs [28]: (a) The shell-correction energies $M_{\text{exp}} - M_{\text{macro}}$ MeV; solid circles denote experimental data (• N–$Z = 48$); x's denote calculations [18]; (b) The fission barriers $[B_{\text{macro}} - (M_{\text{exp}} - M_{\text{macro}})]$; solid circles denote experimental data, pluses shell-corrected data; open circles macroscopic data [25].

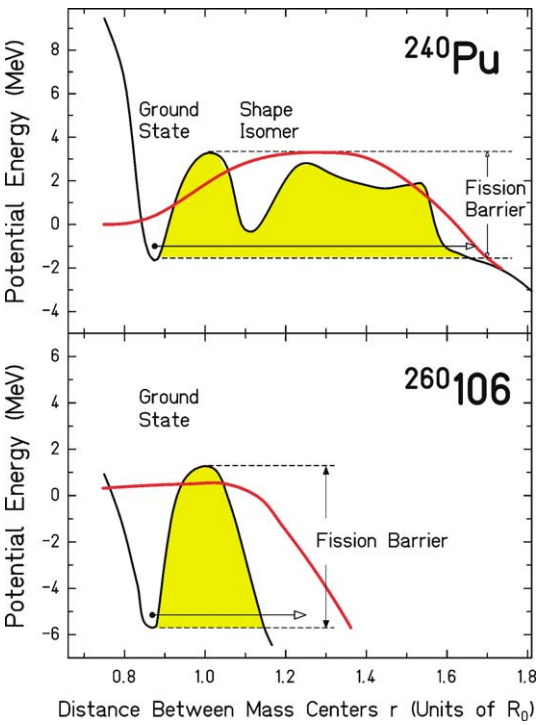

Fig. 4. Comparison of the fission barriers of ^{240}Pu and ^{260}Sg. The narrow, single-humped barrier protects the nucleus ^{260}Sg [18] at small deformations that correspond to the first barrier of ^{240}Pu [29].

barriers for ^{240}Pu [29] and ^{260}Sg [18]. The figure demonstrates that ^{260}Sg has a single high and narrow barrier corroborating the analysis of spontaneous fission half-lives, which indicated large barrier curvature values for the heaviest isotopes [22]. The barrier exit point for ^{260}Sg at 1.15 times the nuclear radius R_0 corresponds to an elongation of about 2.3 fm compared to the diameter of the equivalent sphere of 15.5 fm. The shell stabilization of SHE is restricted to a rather compact configuration close to the 2 : 1 axis ratio of superdeformation. SHE are not only purely shell-stabilized, but also restricted in the deformation coordinate to small elongations of 2 fm only. At larger deformations the superheavy nucleus looses its stability and becomes an ordinary macroscopic droplet.

2.2. Shell corrections from the macroscopic–microscopic approach

Macroscopic nuclear models combined with a microscopic approach, which takes into account the structure of the nuclear system, reproduce best the binding-energies, decay-modes, level-schemes and shell closures in the mass regions that have been studied so far. The most reliable calculations stem from the Warsaw-group for e–e-nuclei of elements $Z = 102$–112 [30]. They reproduce the measured mass-excesses and spontaneous fission half-lives. Fig. 5 shows the shell-correction energies between Pb and element 120 [31]. Extrema of shell corrections are predicted for the deformed nucleus $^{270}_{162}$Hs and the spherical nucleus $^{298}_{184}$114. The landscape between the smallest values near $A = 228$ and the next doubly closed deformed shell at $Z = 108$ and $N = 162$ describes well the trend of the experimental shell corrections, as shown before in Fig. 3(a). A smooth transition to larger negative shell corrections for nuclei approaching ^{270}Hs is predicted, followed by a flat local elevation of 1.5 MeV at $^{284}114_{170}$ between the deformed and spherical minima. Ever shorter half-lives end the periodic system of elements at proton number $Z = 122/124$ due to α-decay and at neutron number $N = 186/190$ due to spontaneous fission. Following the calculations of Fig. 5, the number of superheavy isotopes is as large as the number of stable ones. The world of superheavy elements is no island. It is connected to the world of stable isotopes via the corridor $N–Z = 50 \pm 3$. Long α-chains of odd mass isotopes avoiding spontaneously fissioning e–e isotopes find a way from the superheavy elements to the lighter, long-lived actinides by passing the remainder of a swamp of fission around Rf. The lighter actinides finally decay via the primordial α-chains to the stable isotopes of Pb and Bi, which were used to create the SHE.

The mutual support of shell corrections for neutrons and protons is evident from data on neutron- and proton-binding energies as well as on α-decay Q-values, but is not an ingredient of the macroscopic–microscopic models [32]. A mass formula that takes these findings into account still has high predictive power for nuclei up to the region of superheavy elements [33]. It reproduces best the mass-excess data of the chain $N–Z = 48$ [24] and meets within 0.7 MeV the mass-excess value of 119.6 ± 0.2 MeV at ^{264}Hs.

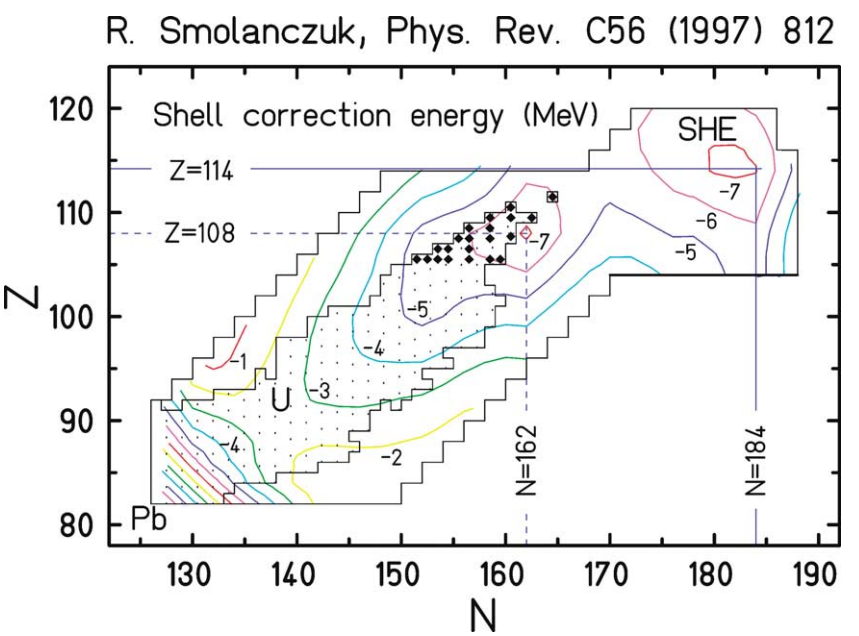

Fig. 5. Shell-correction energies for elements between Pb and element $Z = 120$ [31]. The black symbols are known nuclei beyond Sg.

2.3. Self-consistent mean field theories

Self-consistent mean field models were developed in parallel to the macrosopic-microscopic shell correction method [34–41]. In the last years they reached an accuracy that made them competitive to the shell-correction method [42–48]. The latter is still the more accurate method to extrapolate the bulk properties of nuclei to a nearby neighborhood. This is because, as data accumulated from many experiments, the parameter-sets of the macroscopic–microscopic models were continuously improved.

For extrapolations to regions far from nuclear stability, the different self-consistent mean field models are in principle the better approach. An effective nuclear two-body interaction introduced by Skyrme in 1959 [34] made Hartree-Fock calculations tractable, as was shown by Vautherin and Brink [35–37]. Models using Skyrme-forces (SHF) are a first class of nonrelativistic self-consistent mean field theories, which are applied with varying parameters by different schools [42,43], as discussed in a recent publication [47]. Dechargé and Gogny introduced a two-body force of finite range [39], which required large numerical calculational efforts, but gave very good agreement with nuclear data and level schemes. A second class of self-consistent mean field models are the relativistic mean field, (RMF)-models [41,45]. The finite range interaction is built up from effective mesonic fields, and the spin-orbit interaction in nuclei emerges directly, as was shown back in 1956 by H.P. Dürr [40]. To explain the shell-closures in nuclei, spin-orbit splitting was introduced into the early shell model, into the macroscopic–microscopic approach, and into other SHF-models ad-hoc. The RMF-models predict shell closures far from the region of known nuclei in a unique and direct way. Spin-orbit splitting follows from the gradient of the effective mesonic interaction, which peaks at the nuclear surface. For a given proton shell, the different isotopes show different neutron densities, radii and diffusenesses, which change the spin-orbit interaction. The mutual support of shell closures for neutrons and protons becomes an intrinsic feature of RMF-models. For SHF-models with effective spin-orbit interactions the mutual support is also guaranteed, but the isotopic and isotonic dependences were found to differ from RMF-results. Because shell closures are a direct consequence of the mesonic fields, RMF-models are best suited to answer the question of where the next spherical shell should be expected. For heavy nuclides with large values of isospin, the radial density dependences may adjust such that neutrons and protons have different distributions, or that the nucleon density changes radially. Then the gradient of the potential changes, the spin-orbit interaction adjusts, and the shells are modified. Neutron-rich heavy nuclides far from the known isotopes may have shell closures, which escape description by a macroscopic–microscopic model.

Recent publications reporting results from self-consistent mean field models [42–46] made predictions of the nuclear structure of superheavy isotopes, and of shell-closures beyond ^{208}Pb. Most of the predictions of the macroscopic–microscopic approaches were confirmed. Among them, the deformed shell at ^{270}Hs, a transition from deformed to spherical nuclei for $N = 170 \pm 2$, and a spherical shell at $N = 184$ were found in all calculations. The spherical shell at $Z = 114$ was not confirmed. It moved to $Z = 120$. At $N = 172$ a new sub-shell was found and a new spherical shell closure for $^{292}_{172}120$ is predicted [44,46]. This nucleus is predicted to be a new nuclear species, with a density that is depleted in the central region.

The shell at $Z = 114$ disappears in the self-consistent model using the Gogny-force [46], in RMF models, and in all but one of the SHF-models [47]. The disappearance of the shell at $Z = 114$ is correlated to the size of the spin-orbit splitting of the proton 2f orbitals. In former nonself-consistent models the spin-orbit interaction was fitted to the $p_{3/2}/p_{1/2}$-splitting in ^{16}O. This condition is necessary, but not sufficient. The high spin-orbit doublets also must be reproduced by an interaction that is used to extrapolate beyond known nuclei. The fits reproducing the spin-orbit splitting in ^{16}O overestimated the splittings of the higher 2d- and 2f-orbitals in ^{208}Pb by 50% compared to the experimental values. By far the smallest deviations from the experimental splittings in ^{208}Pb are obtained by the RMF-models. Here, the fit to ^{16}O also reproduces the higher orbits within 20%. Large spin-orbit splittings of the proton 3p- and 2f-orbits favor a shell closure at $Z = 114$, whereas a reduced splitting favors $Z = 120$, as calculated from RMF-models. The good description of the spin-orbit splittings in ^{208}Pb provides a strong argument to switch the search to $Z = 120$, as recommended in [47] and to abandon hope for a shell at $Z = 114$, on which experimentalists have been fixed since 1966. Predictions of the macroscopic–microscopic model [31], such as those shown in Fig. 5, rely on a $Z = 114$-shell. Thus beyond $Z = 112$ they may have to be revised.

A shell closure at $Z = 126$ is predicted by some of the SHF-models with large spin-orbit splittings of the 3p- and 2f-orbits and a high lying $i_{11/2}$-orbit [42], but none of the RMF-models predicts such a shell. Moreover, the α-half-lives of isotopes of elements beyond 122 are predicted to be shorter than the limits set by experimental techniques.

The RMF-models [47], some of the SHF-models [44], and the self-consistent mean field model using the Gogny-force [46] predict a central depletion of the radial density distribution of up to 30%. This central depletion affects the low ℓ-orbits (3p and 2d), which are concentrated in the center of the nucleus, more than the higher ℓ-orbits (2f and 2g) concentrated at the surface. As the gradients of the density distribution at the outer surface and the inner surface change sign, so does the spin-orbit interaction which is proportional to the gradient. The spin-orbit interaction of the 3p- and 2d-orbits defined by the radial interaction integral is strongly decreased, whereas the integral is changed only a little for the 2f- and 2g-orbits. The central depletion is largest when the action of the $N = 172$ and the $Z = 120$ shells support each other, and the shell-gap becomes largest for $^{292}_{172}120$. The RMF-models predict not only a decrease of the spin-orbit splitting, but even a change of the level ordering. $d_{5/2}$ neutrons and $p_{3/2}$-protons should have lower binding energies than their low spin counterparts. The finite range of the

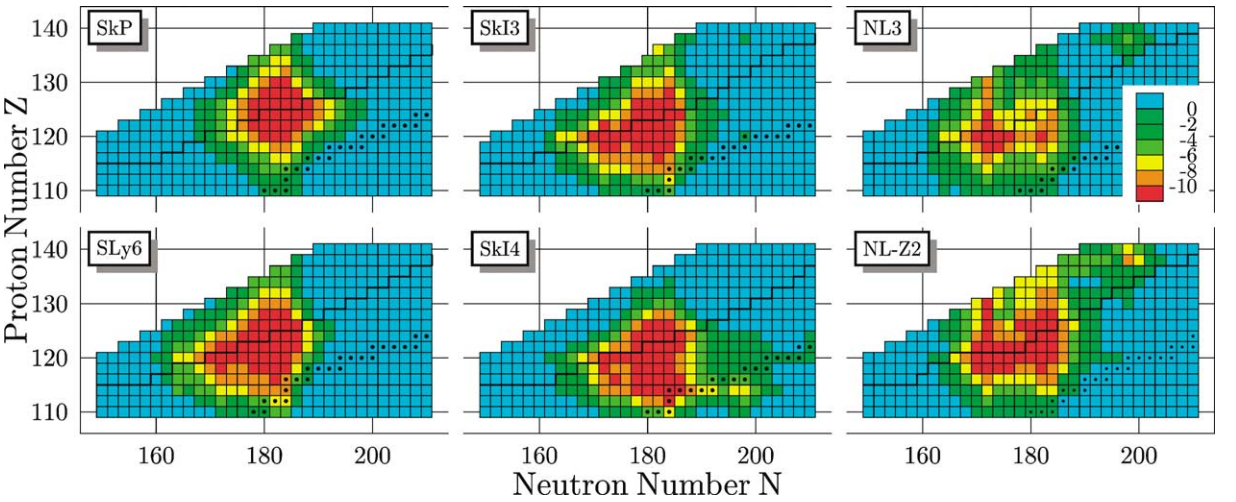

Fig. 6. Representation of shell correction energies summarizing the results of different RMF- and SHF-calculations, as they were in 2001 [47].

Gogny-force [46] combined with a spin-orbit interaction added ad-hoc, treated in a self-consistent calculation, also predicts the central depletion for exactly the same nucleus $^{292}_{172}120$. This cross check of two theories gives additional weight to the prediction.

$N = 172$ is close to the transition to deformed nuclei. Very recent calculations including deformation close to $^{292}120_{172}$ show oblate shapes of the ground states for $N = 172$-nuclei. Whether oblate shapes and spherical nuclei centrally depleted in density coexist in this range, or deformation finally prevails over sphericity once more, is still an open question [48].

Summarizing the results of self-consistent mean field theories: low spin states are found for $Z = 114$–126 as well as for $N = 172$–184, imbedded below and above these numbers in high spin states. All over this (Z, N)-range centered around $^{298}120_{178}$ level densities are small, and shell corrections are large. An extended highly shell-stabilised island of spherical nuclei is to be expected around $Z = 120$ and $N = 178$. Fig. 6 shows a representation taken from [47]. It summarizes the results of different efforts comprehensively, as they were in 2001.

The central nucleus $^{298}120$ could be reached via the 4n-channel in asymmetric reactions of the heaviest e–e actinides and n-rich stable isotopes of the elements $Z = 24$–30. The same beams which gave us the elements $Z = 107$–112 combined with actinides hit the center of spherical SHE. Moreover, the $N–Z = 58$ decay chain is predicted by the different theoretical models. Even symmetric reactions of 2 deformed ^{150}Nd-nuclei reach $^{298}120$ in a 2n-channel. About 2/3 of the combinations of n-rich e–e isotopes covering the whole range of asymmetries offer a landing at $Z = 120$ in the optimal range of $N = 178 \pm 2$. Never a SHE-landing place was better situated than this target. You know where to hit, and you know what calculations want you to find. The announcement of a discovery of element 120 is on the agenda of the coming years. It will need the highest standards of the art of experimentation to show that this wanted and welcome result might be wrong. A difficult task, but I am confident, truth in science finally will not be hidden. In the following discussion on the 'Making of the Elements', it will be shown that the making of SHE is blocked long before element $Z = 120$ is in reach.

3. The making of the elements – a process intrinsically frustrated

3.1. Complete fusion cross sections

Two methods have been successfully used to produce heavy elements beyond nobelium by fusion of two lighter nuclei via xn-evaporation channels: Actinide-based 4n and 5n reactions at excitation energies in the range of 40–50 MeV and Pb/Bi-based reactions in the range of 10–20 MeV. For each of the two methods excitation functions have been measured, except the respective last reactions leading to $Z = 108$ and $Z = 111, 112$.

Fig. 7 shows 5 production cross sections of ^{248}Cm-induced synthesis reactions for elements between Lr and Hs, that is for projectiles between ^{15}N and ^{26}Mg. Hs was reached recently in the reaction ^{248}Cm(^{26}Mg, 5n)^{269}Hs with $\sigma = (6^{+6}_{-3})$ pb [49]. A decrease covering 5 elements of a factor 2×10^3 is observed and a mean factor of 7 is lost going to the next higher element. Extrapolating to $Z = 110$ gives $\sigma = 0.1$ pb. For an element given all lighter actinide-targets show smaller cross sections than ^{248}Cm. Moreover, Fig. 7 shows, that synthesizing elements between No and Hs by 5n-reactions in irradiations of the heaviest e–e targets with ^{26}Mg-projectiles gave cross sections, which decreased by more than 3 orders of magnitude. Going to the next

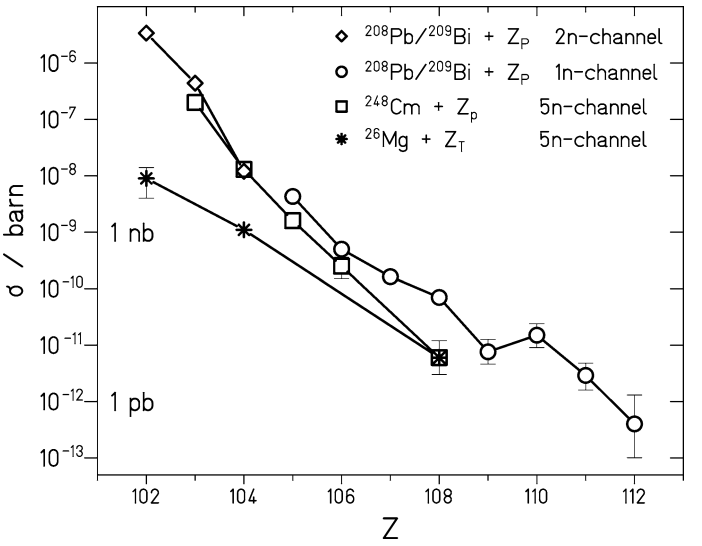

Fig. 7. The highest xn-production cross sections: Pb/Bi-based reactions 1(a) for elements $Z = 102-104$ ($x = 2$), 1(b) $Z = 105-112$ ($x = 1$), actinide-based reactions 2(a) using ^{248}Cm-targets for elements 103–108 ($x = 5$) and 2(b) ^{26}Mg-projectiles for elements 102–108 ($x = 5$).

higher element and keeping the same projectile is paid by a loss factor in the cross section of about 4. In the reaction ^{249}Cf(^{27}Al, 5n)^{271}111 element 111 should be reached at the 0.1 pb-level.

The Pb/Bi-based reactions shown in Fig. 7 cover the range between No and $Z = 112$, that is reactions using projectiles between ^{48}Ca and ^{70}Zn [50,51]. 2n-channels are the strongest channels for $Z \leqslant 104$ and 1n-channels prevail for all higher elements. For the1n-channel a decrease covering 11 elements of a factor 6×10^5 is observed and a mean factor of 3.8 is lost going to the next higher element. Extrapolating to $Z = 113$ gives for the reaction ^{209}Bi(^{70}Zn,1n)^{278}113 a cross section at the 0.1 pb-level.

Starting with Sg the cross sections using the 1n-channel reactions in Pb/Bi-based reactions are larger than the 5n-channel reactions using the heaviest targets. Extrapolations to the 0.1 pb-level are accurate within a factor of 3. For actinide-based reactions we obtain for this level given by the state of the art of foreseeable experiments, an end of element synthesis at $Z = 110, 111$. For Pb/Bi-based reactions $Z = 112, 113$ will be the highest atomic numbers reached in our search.

Fig. 7 presents the essence of 20 years of most sophisticated reaction studies using chemical methods and recoil separation techniques. We learnt going to the next higher element, we are charged to pay a good factor, as cross sections decrease exponentially. Using actinides to produce $Z = 120$ we estimate a cross section of 10^{-45} cm^2. A realistic goal is to reach $Z = 110$ by the reactions (^{244}Pu + ^{36}S) and (^{248}Cm + ^{30}Si) giving in the 5n channel the $N = 165$ and 163 isotopes of element 110, an extrapolation following directly from the experiments presented in Fig. 7.

The two production methods demonstrated in Fig. 7 seem to indicate a slight advantage for the Pb/Bi-based method. Comparing the reactions leading to $Z = 108$ the factor between the σ-values for production of ^{265}Hs and ^{269}Hs is within an order of magnitude, a marginal difference in the scale of cross sections covered from 10^{-25} cm^2 to 10^{-37} cm^2, but important and decisive at the limit of making or not making a new element at the border of the table of elements. A comparison of cross sections in the 10 nb-range producing the same isotope of an element by the two methods is possible for ^{253}No and ^{254}Lr. A factor of 15 in favour of the 3n-channel for the (Pb/Bi + ^{48}Ca)-reactions in respect to the 5n-channel in (^{232}Th + ^{26}Mg, ^{27}Al)-reactions has been reported [52–54]. There is again the small advantage for the colder 3n-channel compared to the 5n-channel. To explain the difference is a challenge, as the many stages of the formation process have to be understood quantitatively in order to get the factor right. We are still far from that. But empirically, we can state an advantage for the Pb/Bi-method of about an order of magnitude, which may result in reaching higher atomic numbers by this method. The gain may be one or two atomic numbers, which from a general point of view is marginal. Following the analysis of the cross sections shown, the present experimental limit of detection of one atom/month, irrespectively of the method used, will stop us at $Z = 112 \pm 1$. To extrapolate our most reliable experiments as a guide to the next step is a responsible action, guarantees a high chance success, and saves money. At GSI this strategy was applied. But few have fun to do it this way.

Investigating symmetric collision systems we cover the critical range of fissilities $x > 0.72$ for compound systems with $Z < 92$. The fission losses in this element range are much smaller than for elements above $Z > 92$. xn-channels are populated with cross sections (10^{-26}–10^{-32}) cm^2, which allow for measurements of excitation functions. Those are an indispensable help for heavy element synthesis. An extensive experimental program was launched and accomplished in the UNILAC-period

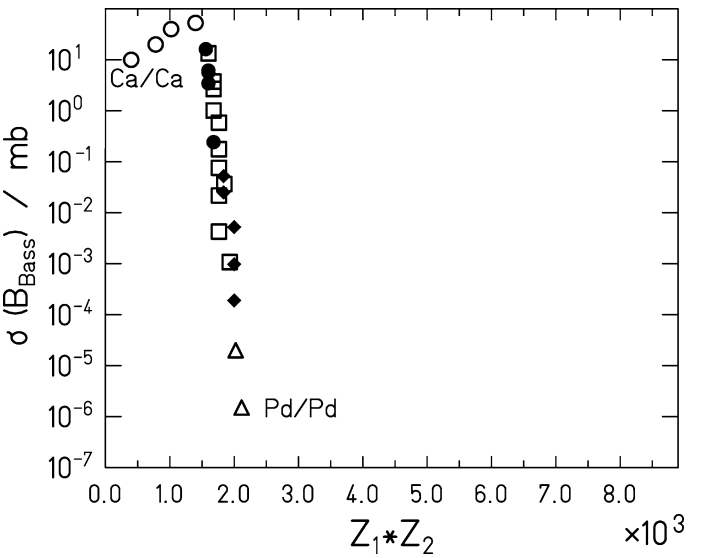

Fig. 8. Evaporation residues cross-sections at the Bass-barrier for nearly symmetric collision systems. Circles indicate data from [56]; diamonds, from [57]; squares, from [58]; triangles, from [59]. The heaviest combinations of collision partners reach $Z_1 Z_2 = 8800$.

(1978–1988) [55–59]. Fig. 8 presents the cross sections for nearly-symmetric collision systems. The cross sections are given at the Bass-barrier [60]. Between $Z_1 \times Z_2 = 1600$ and 2100 the σ-values drop by 7 orders of magnitude passing the range of compound systems between $Z = 82-92$. Below this range, fusion shows σ-values up to 100 mb. Above this range we enter the nb-regime, and we may reach σ-values at the 0.1 pb-level for $Z = 94$. For $Z_1 \times Z_2$-values between 2200 and 8800 reached at (U + Cm), that is, for half of all collision systems, fusion of symmetric systems is not detectable. The disappearance of complete fusion occurs within a range of 12 elements with a loss factor of 5 going from one element to the next. The exponential break-down, demonstrated in Fig. 7 for the synthesis reactions of the heaviest elements, is observed also within the same range of elements. The loss factor of 3.8 for 1n-reactions increases to values of 5 and 7 for 4n-(symmetric) and 5n-channels (^{248}Cm), respectively. Such a trend to larger exponential slopes is also observed going from 1n- to 3n-channels in Pb/Bi-based reactions [1,51].

Of special interest to understand the limits of element synthesis are observations at the limit of disappearing EVR-formation. Fig. 9 shows total EVR-cross sections for the symmetric collision systems between (^{100}Mo + ^{100}Mo) and (^{110}Pd + ^{110}Pd) giving compound nuclei between ^{200}Po^{x} and ^{220}U^{x} [55,58,59]. The excitation functions shown start near the barrier which is indicated and reach saturation at energies far above the barrier. A gap of 8 atomic numbers ($Z = 84$–92) at fissilities between 0.73 and 0.80 has been covered by these experiments. Cross sections for all reaction channels in a range of excitation energies up to 80 MeV were measured by applying EVR-α-chain analysis for all detected short-lived α-emitters. The different xn-, (yp,xn)- and ($z\alpha$,yp,xn)-channels could be separated. Excitation functions were analysed and helped to assign the isotopes. Most important were the heaviest collision systems ^{104}Ru + ^{110}Pd $\rightarrow$ ^{214}Th^{x} and ^{110}Pd + ^{110}Pd $\rightarrow$ ^{220}U^{x} with cross sections below the μb-range. Decay channels were identified down to a level of 0.1 nb [59]. All in all, in our investigations, cross sections spanning 8 orders of magnitude were scanned. This range equals the range of production cross sections observed in the synthesis of elements $Z > 102$ from 10 μb to 0.1 pb, but at a level of 10^3 times higher cross sections, as the compound nuclei situated in regions 4 and 5 of Fig. 2, are protected against fission losses by broad and high fission barriers.

Fig. 10 presents the element distribution observed for the three heaviest systems shown in Fig. 9 at about 40 MeV excitation energy [59]. This is the energy range covered by 3n- to 5n-channels, important as well for actinide-based synthesis reactions. The measurements are compared with HIVAP-simulations [61]. At $Z = 88$ good agreement is observed, but already at $Z = 90$ the xn-channels observed are found to be reduced by an order of magnitude compared to the simulation. Such a dominance of α-channels was observed already earlier for lighter systems [62]. Finally, at $Z = 92$ no xn- and pxn-channels could be identified, and even the αxn-channels reach only 7% of the expected value. In the Pd/Pd-system the highest element observed is not U, but Th. Fusion rapidly within two atomic numbers becomes incomplete. Precompound α-emission makes the residues of U and Pa disappear. The main flux in the reaction goes to Ra, not to U. Very recently the rapid disappearance of xn- and pxn-channels was observed also in JAERI-experiments [63] investigating the system ^{82}Se + ^{150}Nd $\rightarrow$ ^{232}Pu^{x} at an effective fissility of the compound system of 0.79, that is close to the case of Pd/Pd. Within a few nb U-isotopes are reported to be seen,

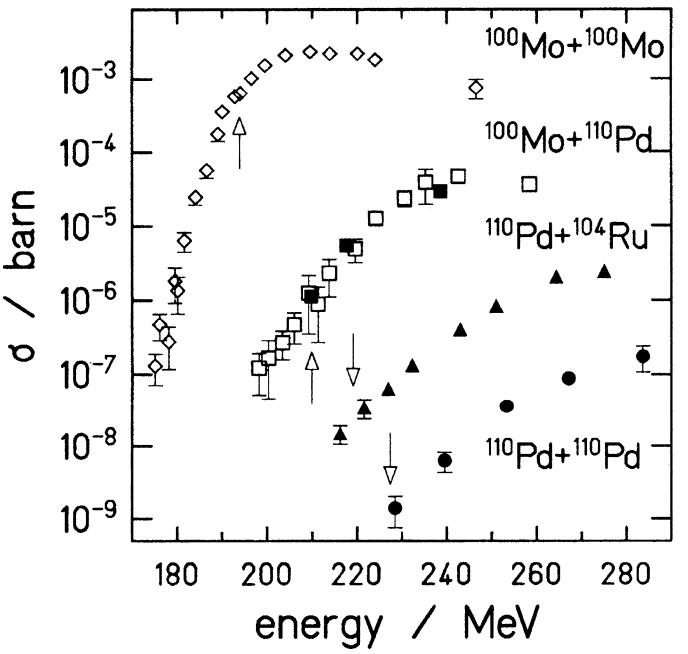

Fig. 9. Total evaporation-residue cross sections for the systems indicated [59] (full symbols) and from [58] (open symbols) as function of center-of-mass energy. The arrow indicate the Bass barriers of the systems.

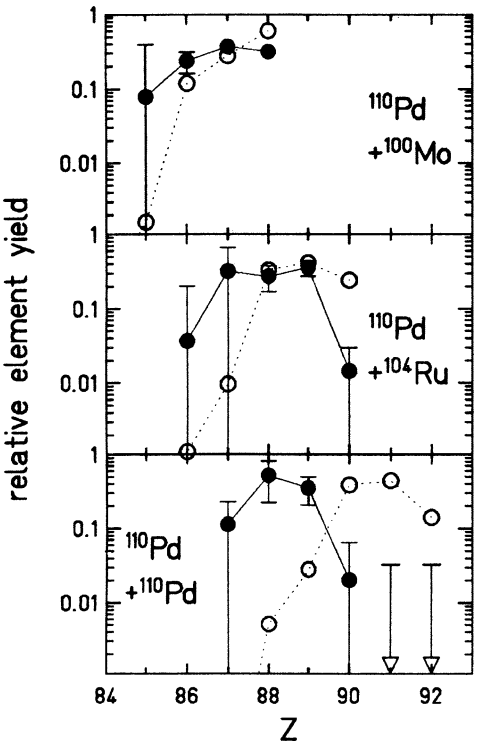

Fig. 10. Relative element distributions from experiment (full points) and HIVAP calculation (open points and dotted lines) for the indicated systems around 40 MeV excitation energy [59]. The arrows indicate upper limits. The element yields are normalized to the sum over all measured elements.

but no Pu- or Np-isotopes were detected at a nb-level. Two atomic numbers less in the system ^{76}Ge/^{150}Nd [64] xn-channels were still observed, as in the system ^{110}Pd/^{104}Ru.

Emitting precompound α-particles brings the system to a nucleus with a higher fission barrier, which is situated at a more elongated deformation. Such a system is better stabilized against fission and the distance it had to pass between the binary configuration in close-approach (see Fig. 11) and the fission barrier of the mono-system is reduced. The formation probability of the Z–2-nucleus and its chance to survive fission, both are increased [59]. For the two systems showing the loss of xn-channels it would be desirable to push the detection limit to the pb-level in order to measure the loss factor for xn-channels down to the limiting fissilities. σ-values for more asymmetric fusion reactions using targets between Nd and Pb are important, but all these experiments at low cross sections are lengthy and will not be easy.

Until now for actinide-based reactions a dominance of α-channels was never observed. But, we cannot exclude that at the limits ($x > 0.80$) the phenomenon could also become of importance in SHE-synthesis, even if the arguments to explain the α-dominance given above for lighter system may not hold for SHE. Both the positions of the binary configuration in close-approach and of the fission barrier of the compound system for SHE are less Z-dependant than for the lighter elements discussed. The distance to be overcome in fusion is hardly Z-dependant. Precompound α-emission certainly decreases the disrupting Coulomb forces in the amalgamation stage for all elements. However, the reduction of the fissility in this stage has not yet been considered quantitatively for incomplete fusion reactions.

3.2. The stages of fusion

To organize the following discussions we present the different stages of the fusion process first, Fig. 11. To each of the 4 stages a probability may be attributed to pass to the next stage. The total production cross section σ_{EVR} is the product of four factors. To react at an angular momentum ℓ_{lim} at all is the basic first factor, $\pi\lambda\!\!\!^{-2}\ell_{\mathrm{lim}}^2 = 5{-}50$ mb with $\lambda\!\!\!^{-}$ the reduced wave-length and $\ell_{\mathrm{lim}} = 15$ for a synthesis of highly fissionable nuclei. The probability to reach the pocket of the potential $\mathrm{p}_1(x, \mathrm{B_B}, \mathrm{E_{cm}})$ in a close-approach stage depends on x the effective fissility during the passage, scaling the depth of the potential pocket, the

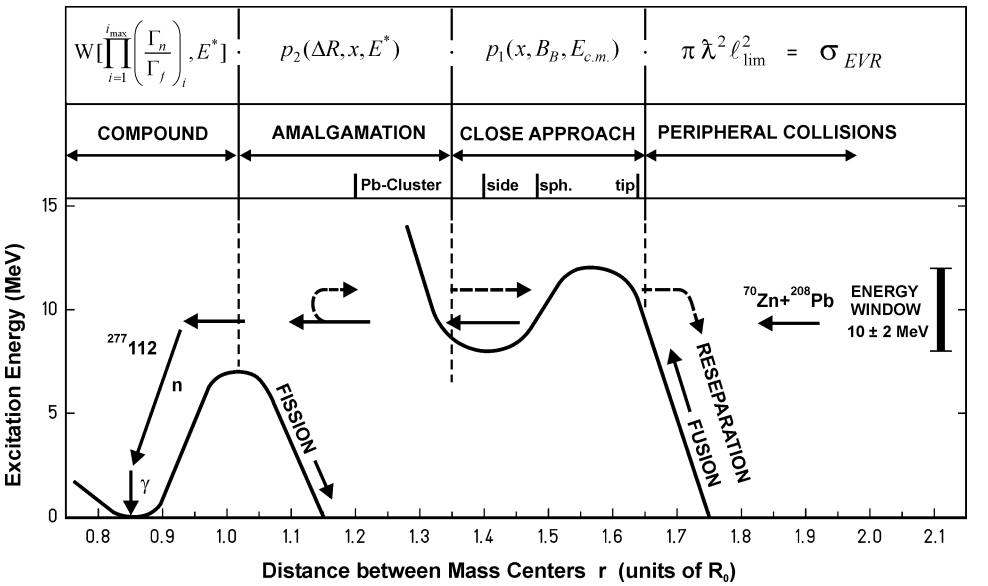

Fig. 11. Stages of the fusion path towards element 112 for the ^{70}Zn/^{208}Pb collision system [65]. The 4-factor presentation of the different stages is explained in the text.

kinetic energy in the c.m. system, and the height of the fusion barrier B_B. To pass further to the inner fission barrier of the final product gives a factor $p_2\ (x, \Delta R, E^*)$ depending on $x, \Delta R$ the distance to be bridged, and the excitation energy E^*. The last factor $W(\Pi(\Gamma_n/\Gamma_f)_i, E^*)$ concerns the deexcitation of the compound nucleus governed by the excitation energy E^* and the product of (Γ_n/Γ_f)-values in the various deexcitation steps. The product of the last 3 factors for a reaction with no fission losses and unhindered fusion saturates at 1, whereas for a reaction at the 0.1 pb-level the product is as small as 10^{-11}. To calculate a reaction branch of 10^{-3}, that is a σ-value on the 10 µb-level, is state of the art in fission and heavy-ion reaction theories. But an accuracy of 10^{-11} for a multistep-reaction with different physics in each step, is far beyond what theories can do today. The great theoretical success, giving consistent results for the ground state properties of SHE and their decay modes, as presented in Section 2, has no counterpart in predicting reaction cross sections at a pb-scale. To understand trends and to find the physics behind the exponential decrease in production probabilities was, and still is, the main help theory can give to experiments to date.

The distance R between the colliding partners is measured in units of the radius R_0 of a spherical final product. The ground state of a spherical nucleus is positioned at $R/R_0 = 0.75$. A deformed ground-state is found at about $R/R_0 = 0.85$. The fission barrier of a deformed SHE is close to $R/R_0 < 1.1$. The close-approach stage of collision partners is found in the range $R/R_0 = 1.4$–1.65 with spherical partners at $R/R_0 = 1.5$. A spherical projectile like ^{26}Mg may hit a prolate target nucleus at the tip ($R/R_0 = 1.65$ or at the side $R/R_0 = 1.4$. At $R/R_0 = 1.8$–2.0 nuclei begin to interact. In the example chosen, the excitation energy of 10 ± 2 MeV fits to an 1n-channel, as observed, e.g., in ^{208}Pb(^{70}Zn, 1n)^{277}112. The barrier, as presented is taken from [65]. In each of the stages the systems either proceed to smaller R/R_0-values or reseparate. Finally, in the last stage a neutron is emitted, either in compound deexcitation or as a precompound neutron. The remaining excitation energy is small, and the SHE is protected behind its fission barrier.

The close-approach stage as a starting configuration of the amalgamation stage, has recently been treated in a comprehensive new calculation presented by V.Yu. Denisov and W. Nörenberg [65], which compares also to previous models. For different collision systems with spherical or deformed partners, the fusion barrier and the depth of the pocket are calculated together with their positions. Now, the close-approach stage as well as the compound stage are well defined,. It is a step forward to see the boundaries of the amalgamation stage fixed, discarding the use of any fissility. The crucial question how to pass the gap of 4 fm, equal to twice the barrier deformation of SHE, remains the open task of the future.

3.3. An effective fissility for fusion and the 'Coulomb Falls'

For fusion reactions a macroscopic scaling parameter in the spirit of N. Bohr's fissility was formulated by J. Blocki et al. [66]. A measure of the ratio of the macroscopic Coulomb and surface forces for a nuclear monosystem is the classical fissility $x_0 = (Z \times f(I)/101.8)$. It is proportional to Z, the atomic number of the nucleus, and to a function $f(I) = (1-I)/(1-1.78I^2)$, where $I = (N - Z)/(N + Z)$. For the heaviest nuclei accessible by fusion, this function is nearly constant with a value close

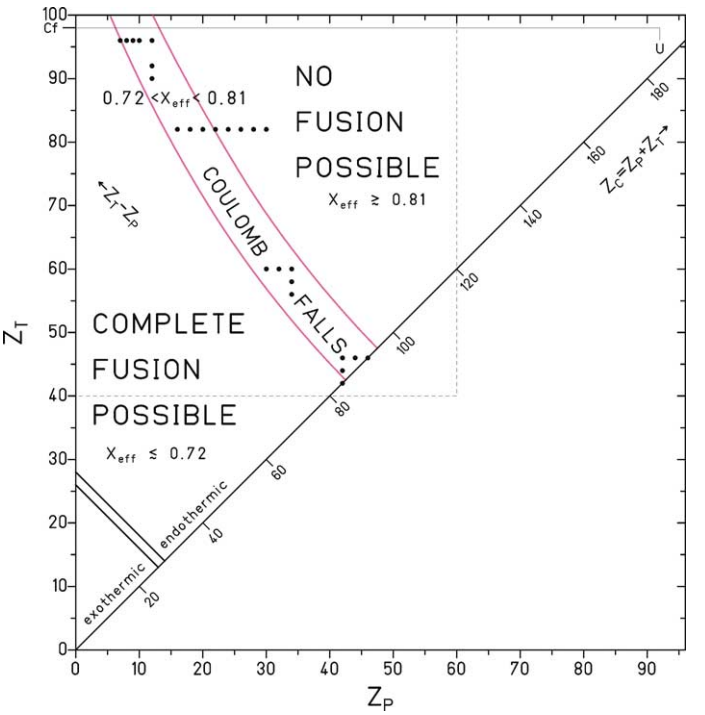

Fig. 12. The triangle of Z_T/Z_p-combinations of available collision partners. xn-cross sections break down from 10^{-26} cm^2 to 10^{-37} cm^2 in the 'Coulomb Falls', which separates systems which fuse and systems which do not fuse. The lines of constant effective fissility $x = 0.72$ and $x = 0.81$ are indicated. Dots show systems in the 'Coulomb Falls' the fusion of which has been detected and which are discussed in the text.

to 0.86. For a binary system of two touching nuclei with equilibrated charge densities, the expression $x_\infty = x_0 \times f(\kappa)$ with $f(\kappa) = 4/(\kappa^2 + \kappa + \kappa^{-1} + \kappa^{-2})$ and $\kappa = (A^1/A^2)^{1/3}$ was derived [66,67]. The term $f(\kappa)$ takes into account the decreasing Coulomb energy between mass-asymmetric collision partners. The effective fissility x of a fusing system is a weighed mean of the fissilities of the mono- and binary system, but it stays proportional to the atomic number Z of the compound system

$$x = \left(\frac{Z}{101.8}\right) \times f(I) \times \left[(1-\alpha) + \alpha f(\kappa)\right].$$

The weight of the binary system α fitted to experimental data is taken as 1/3 [66]. Adding neutrons to the heavy partner helps to reduce x, as expected. Adding neutrons to the light partner may do the contrary. A very asymmetric collision system has, at constant mass of the compound system, a lower x value than a more symmetric one, and this fact neutralizes the decrease of x expected for a higher number of neutrons in the light partner [51]. The effective fissility is a macroscopic scaling parameter ignoring nuclear structure completely.

Fig. 12 shows a diagram presenting all possible combinations of collision partners in fusion, we may combine from stable isotopes of the elements used for targets and beams. The effective fissility x with $\alpha = 1/3$ fixed depends in good approximation for the heavy element synthesis reactions on only two variables, the asymmetry $Z_T - Z_p$ and the atomic number of the synthesized element $Z = Z_T + Z_p$. The lines corresponding to $x = 0.72$ and 0.81 are indicated in the figure. Within a range of $\Delta x = 0.1$ the production cross sections for a fixed heavy collision partner decreases passing about 10 elements by a factor 10^7, as was shown in Figs. 7 and 8. In Fig. 12 are indicated the collision systems with black dots, the cross sections of which were discussed, or will be discussed later. The break-down of fusion demonstrated experimentally was predicted by W. Swiatecki very early [68]. Its discovery is as fundamental as the on-set of its counterpart fission, and to ignore it would be like ignoring the latter. Experiments on deep-inelastic and transfer reactions of heavy ions close to the Coulomb barrier were performed at GSI extensively [69–71]. They independently established the disappearance of fusion in the fissility range above $x = 0.72$. In [69] it was stated that the last partner to fuse with U should be Cl giving $Z = 109$. In the meantime fusion with ^{34}S ($Z = 16$) was found [72], but it could not be detected for ^{40}Ar ($Z = 18$) at an upper limit of 0.6 pb [73]. We still wait for the cross section of the (Cl/U $\rightarrow$ Mt)-reaction.

In my review [51] I called the transition region where fusion rapidly disappears the 'Coulomb Falls', as increasing Coulomb forces in the collision system provoke this drastic change and disappearance of complete fusion. The goal of reaching a

high atomic number $Z = Z_p + Z_T$ is intrinsically frustrated by the increasing Coulomb forces during the formation of the wanted element out of the two collision partners. Beyond the threshold value of the fissility the exponential decrease of the production cross section with Z will be universal. We have given the data for ^{248}Cm, ^{208}Pb/^{209}Bi, and ^{110}Pd as heavy collision partners. Factors of 4 to 7 between the cross sections of neighboring elements were observed. In the future we can hope for a comprehensive data-set to corroborate the universality of the 'Coulomb Falls'. The ground-state properties of the fused systems manifest themselves strongly in the deexcitation of the compound system, but for its formation they seem to be irrelevant. In the 'Coulomb Falls' macroscopic surface- and Coulomb-forces rule the formation and in a diffusion-like process the system passes the long distance to the narrow shell-stabilized region of the compound system. The probability to arrive against growing Z-dependent x-values decreases exponentially and the passage to higher elements is barred. We will show that nuclear structure plays its role in the different stages of fusion. It will not stop, but as is shown in Fig. 12 at $Z_T = 82$ by dots passing the $x > 0.81$ limit, it is able to delay in the case of ^{208}Pb the on-set of the break-down into the 'Coulomb Falls'. In our search for nuclear structure born SHE in any case the naïve hope to go on for ever is finally drowned in the cataract of the 'Coulomb Falls'. This is a hard lesson most of us have a problem to digest.

4. Heavy clusters – nuclear structure supports element synthesis

Nuclei are fascinating objects as nuclear structure gives them complexity, variety, and individuality. But, the energies involved in nuclear structure phenomena are small (<15 MeV) compared to nuclear binding energies and the energies necessary in large rearrangement processes such as fission and fusion. SHE exist by shell correction energies of less than 10 MeV at nuclear binding energies larger than 2 GeV. Evidently, there is nuclear structure in the collision partners of fusion and in the final fused system, but not so evident nuclear structure acts also in the fusion process itself, as will be exemplified in this section.

4.1. Nuclear structure in the compound stage

Certainly, the most important nuclear structure phenomenon in the compound system is the existence of SHE at all. Large shell-corrections protect SHE against fission. Their fission barriers are high and narrow. As was discussed in Section 2, superheavy nuclei may be deformed or spherical in their ground-state.

Fig. 13 shows the nuclear structure of the compound systems in the 'Coulomb Falls'. The coordinate system chosen, asymmetry $Z_T - Z_p$ versus atomic number of the element to be synthesized $Z_T + Z_p$, is orthogonal, but rotated by 45° compared to the presentation of Fig. 12. All systems investigated are indicated.

Compound nuclei between $Z = 96$–112 are deformed. Their deexcitation is well described by simulation codes, e.g., the HIVAP-code [61,74].

Spherical nuclei at $Z = 126$ of the elements between $Z = 88$–92 are synthesized using nearly symmetric collision systems. Here, nuclei have large shell-corrections and are spherical. They are the smaller brothers of spherical SHE (Fig. 2). They show higher fission rates compared to neighboring deformed compound nuclei [20,51]. The competition between n-emission and fission is determined by the level densities and their temperature dependence. At low excitation energies, level densities are different in spherical and deformed nuclei. The concept of collective enhancement of level densities was introduced in 1974 by S. Bjornholm and B. Mottelson [75]. It has become part of the codes simulating deexcitation of compound nuclei [55,76] and is routinely applied in fusion and spallation. Collective enhancement disappears at higher excitation energies and its exponential damping with excitation energy is described in a formalism formulated by A.V. Ignyatuk [77]. To understand the low production rates of the $N = 126$-nuclei in fusion besides collective enhancement, also the geometrical restriction of the ground-state shell corrections to a region of deformation, which is small compared to the extension of the fission barrier of these nuclei, may contribute to the very weak stabilization against fission observed experimentally. The spherical SHE as well are destabilized against fission by collective enhancement of level densities [78]. But this might be without consequences, as produced by collision partners beyond the 'Coulomb Falls' they have been destroyed already before when passing the cataract.

4.2. Nuclear structure in the close-approach stage

Fig. 14 shows the nuclear structure of collision partners involved in fusion reactions leading to elements between $Z = 82$ and $Z = 120$. Between symmetric collision systems at the bottom ($Z_T = Z_p$) and highly asymmetric systems C/Cf at the top, nuclear structure changes several times. There is only one system of two doubly magic nuclei ^{208}Pb/^{48}Ca. Systems with 3 and 2 closed shells in a collision system are indicated by green lines or dots. The strong shells $N = 126$ and $Z = 82$ define together with shells in lighter nuclei $N = 20, 28, 40$ and $Z = 20, 28$ the region 1b, whereas the shells $N = 82, 50$ and $Z = 50$ define region 2b. Stable, n-rich closed shell nuclei of importance in region 1b are ^{208}Pb and ^{209}Bi together with ^{36}S, ^{48}Ca, ^{64}Ni, and ^{70}Zn. In region 2b we find ^{136}Xe, ^{138}Ba, ^{139}La, ^{124}Sn, and ^{86}Kr–^{89}Y. The nuclei between ^{96}Zr and ^{116}Cd are soft, they define

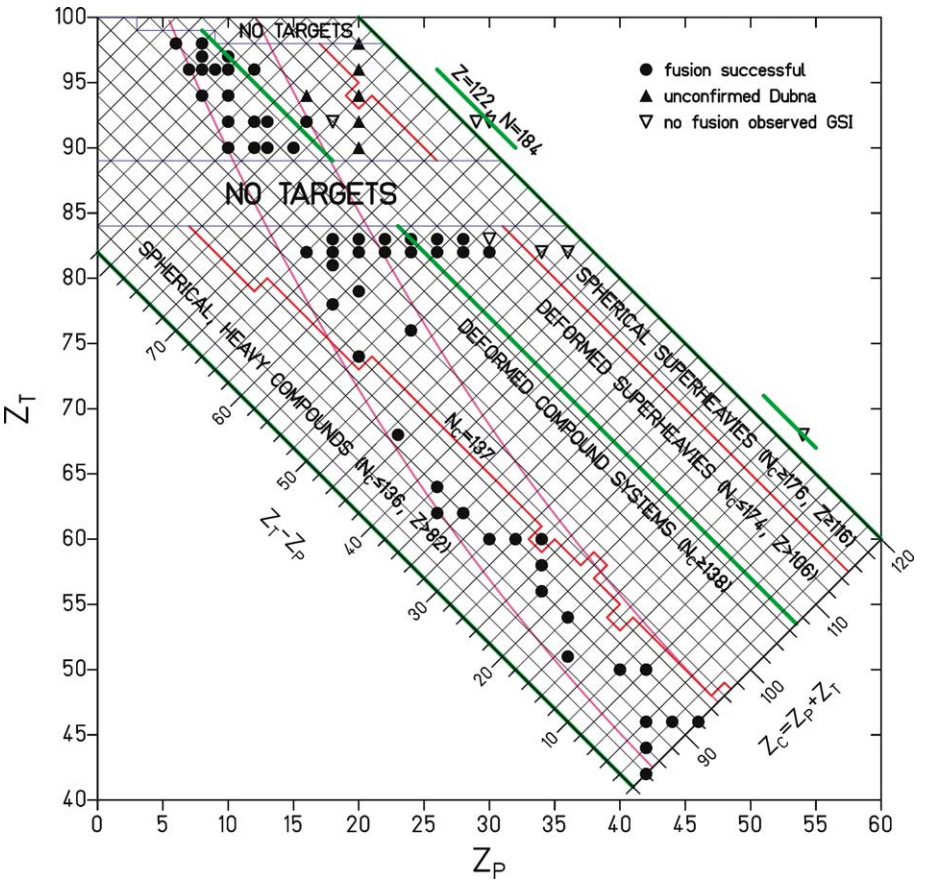

Fig. 13. Compound systems ($Z_T + Z_p$) reached in fusion as a function of asymmetry ($Z_T - Z_p$). The nuclear structure of compound systems in the different regions is indicated. Dots show systems in the 'Coulomb Falls' the fusion of which is detected. The Pb/Bi-based systems giving $Z = 102$–112 are found beyond the $x = 0.81$ line. Unsuccessful reactions and the unconfirmed ^{48}Ca actinide systems beyond $x = 0.80$ are also indicated.

region 3 at symmetric systems. Deformed prolate nuclei are found in region 1a. They are the targets between ^{232}Th and ^{249}Cf in actinide-based reactions. Between ^{150}Nd and ^{192}Os a second large region 2a shows prolate nuclei. Isotopes with a tendency towards oblate shapes are ^{116}Cd and ^{198}Pt at the borders of region 3 and region 2a.

Many studies in support of the experiments on SHE are still missing. They are important and indispensable. Blue lines in Fig. 14 indicate possible investigations passing the 'Coulomb Falls'. In the deformed region 2a the use of ^{192}Os, ^{186}W and ^{154}Sm, ^{150}Nd at the borders and ^{170}Er in the center of this region is proposed. In the spherical region 2b ^{138}Ba and ^{136}Xe-induced reactions should have priority. For the intermediate oblate nuclei ^{198}Pt and ^{116}Cd only the collision system Ar/Pt was investigated [79], and further studies are needed. It would be desirable to systematically pass through the 'Coulomb Falls'. The nuclear structure-dependant entrance and exit fissilities and the number of elements found in the passage should be determined.

The production cross section using deformed targets depends on the angle between the flight path of the colliding projectile and the principal axis of the deformed nucleus. Collisions in direction of the long axis of a prolate nucleus are called tip-collisions, whereas collisions in the plane of the short axes are called side-collisions. The distance between the two touching nuclei is larger for tip collisions than for side-collisions, that is the Coulomb-barrier for tip collisions is lower than for side-collisions. The inverse holds for the excitation energy brought into the system.

In an investigation of the fusion of $^{16}O + ^{238}U \rightarrow ^{254}Fm^*$ ($x = 0.69$) D. Hinde et al. [80] observed that fusion only results from side-collisions, and no fusion was observed in case ^{16}O was hitting the tip of the prolate nucleus ^{228}U. Already at $x = 0.69$ the nuclear structure of ^{238}U started to limit the fusion process, that is well below $x = 0.72$. The systems $^{64}Ni + ^{154}Sm \rightarrow ^{218}Th^*$ ($x = 0.75$) and $^{76}Ge + ^{150}Nd \rightarrow ^{226}U^*$ ($x = 0.77$) were investigated by S. Mitsuoka et al. [81] and K. Nishio et al. [64] at the JAERI-Tandem and RMS-facility. Again, only fusion by side-collisions was observed for both systems. Fig. 15 shows their result for the ^{64}Ni/^{154}Sm-system. The cross sections are plotted against the excitation energy

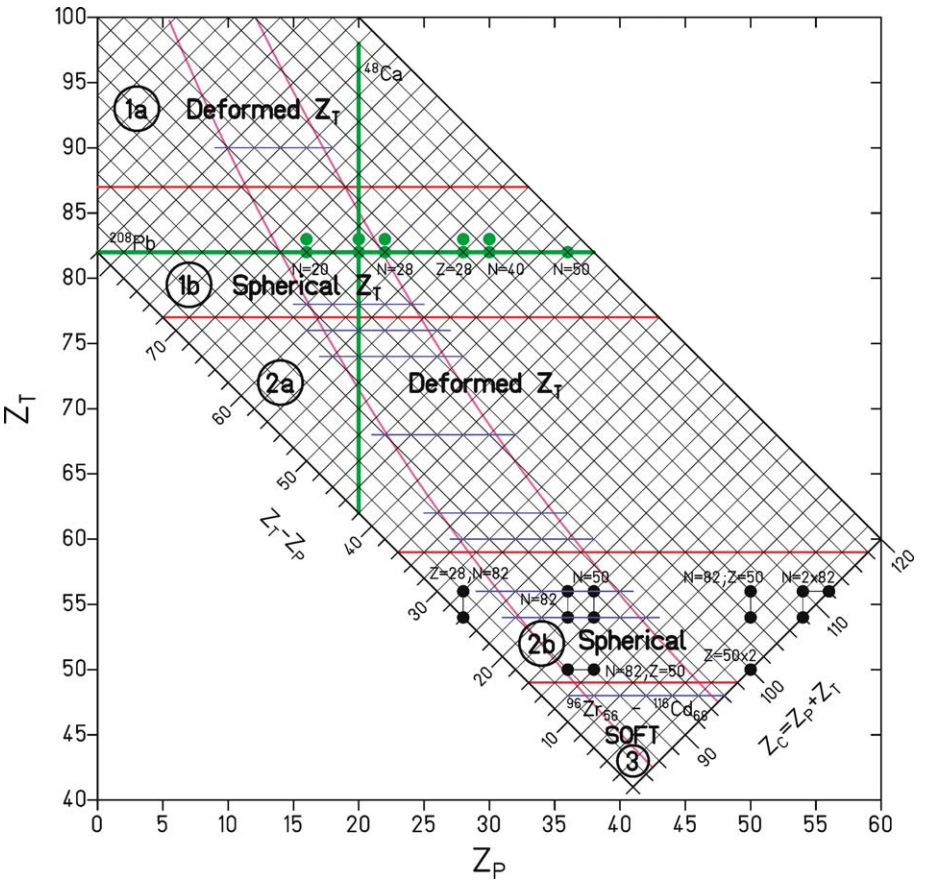

Fig. 14. Compound systems ($Z_T + Z_p$) reached in fusion as a function of asymmetry ($Z_T - Z_p$). The nuclear structure of the heavy collision partners in the different regions is indicated. Systems with at least 2 closed shells are indicated by green lines or dots. Region 1 covers $Z_T = 98$–78 passing from prolate to spherical to oblate target nuclei; region 2 covers in $Z_T = 76$–48 once more the different types of nuclei, as in region 1; region 3 covers in symmetric pairs $Z_T = 40$–46 a range of soft nuclei (^{96}Zr to ^{110}Pd). The use of the heaviest e–e nuclei for fusion is assumed. The passage through the 'Coulomb Falls' is universal and can be studied in all regions (blue lines).

in the system. Compared to a simulation admitting all orientations, the data show a suppression of the 2n- and 3n-channels which correspond to tip-collisions. The 2n-channel was still observed at a level of 4×10^{-3}. The side-collisions populate the higher (4n–6n)-channels which are observed at excitation energies of about 50 MeV. The side-collisions at their smaller touching distance show no hindrance, their channels are open and well transmitted. The result for the ^{76}Ge/^{150}Nd-system at a still higher x-value corroborates the result: also no hindrance for side-collisions and a loss of the 1n- and 2n-channels populated by tip-collisions. Fusion using deformed nuclei starts at higher excitation energies than for spherical nuclei. Their effective Coulomb-barrier is shifted beyond the Bass-barrier, in the language of W. Swiatecki they fuse, but with an extra-push.

For ^{150}Nd-targets three pairs of collision partners were investigated. Below ^{76}Ge/^{150}Nd [64] the system ^{70}Zn + ^{150}Nd $\rightarrow$ ^{220}Th* ($x = 0.75$) was studied by Ch. Stodel et al. at GSI [82]. Excitation functions are shown in Fig. 16(a). The Bass-barrier equivalent to a barrier of a hypothetical spherical ^{150}Nd, falls on the 3n-channel, which is suppressed by a factor of about 4. The 1n- and 2n-channels were detected, but shifted to higher energies and strongly suppressed. The data were analyzed following the extra-push concept. An extra-push derived of 18 MeV is compatible with the cut-off of tip-collisions below 25 MeV allowing still for the remainders of 1n- and 2n-channels. Such remainders were observed no more in the ^{76}Ge/^{150}Nd-system [64]. Going still higher to ^{82}Se + ^{150}Nd $\rightarrow$ ^{232}Pu* ($x = 0.79$) [63], as discussed earlier in the section on cross sections, no xn-channels were observed at all and only a remainder of αxn-channels was observed at the nb-level. At the pb-level xn-channels may still be found and even appear for the pair ^{86}Kr/^{150}Nd $\rightarrow$ ^{236}Cm* ($x = 0.81$).

The result of the above observations transcribed to actinide targets destroys the hope to find low xn-channels. 4n-channels and higher channels are observed and they would be populated in close-approach side collisions. Side collisions give excitation energies above the Bass-barrier and the channels populated are well transmitted. The close-approach distances reached are

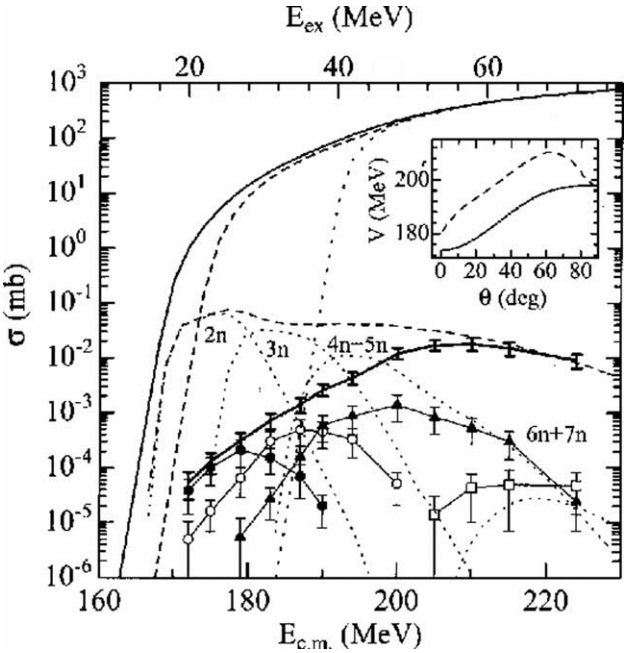

Fig. 15. Measured excitation functions in ^{64}Ni + ^{154}Sm [81] reaction for xn channels (2n, solid circles; 3n, open circles; 4n + 5n, solid triangles; 6n + 7n, open squares). The thick solid curve with error bars and the dashed curve are the sum of the measured and the calculated xn cross sections, respectively. For this system the Bass-barrier [60] is found at $E^* = 38$ MeV (4n-channel), tip collisions at $E^* = 19$ MeV (2n-channel), and side collisions at $E^* = 48$ MeV (5n-channel).

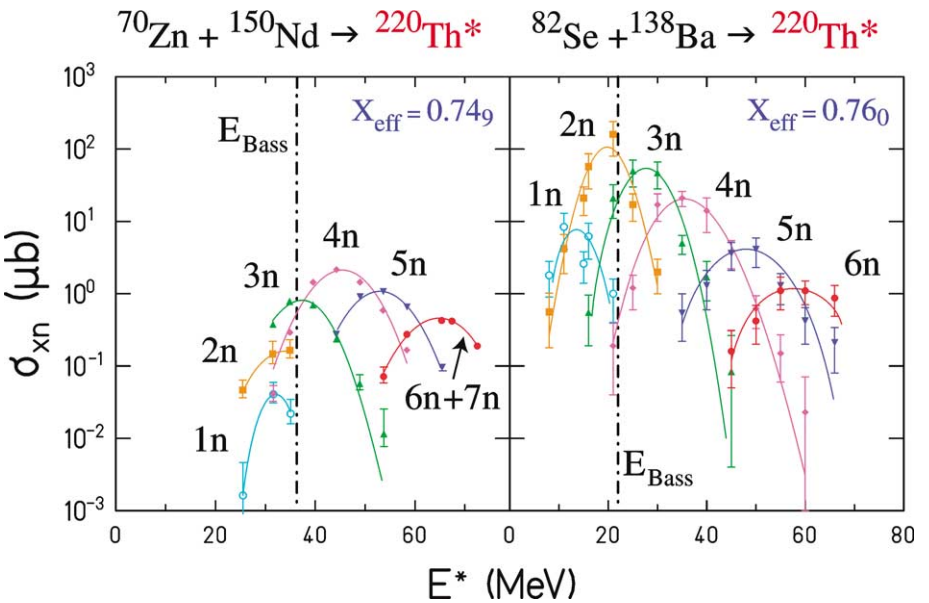

Fig. 16. Excitation functions of xn-channels for the systems ^{70}Zn/^{150}Nd, $x = 0.74$ [82], and ^{82}Se/^{138}Ba, $x = 0.75$ [86], both leading to ^{220}Th*. The first system with the deformed target nucleus ^{150}Nd shows side collisions (4n-channel), whereas the second system with the closed-shell target nucleus $^{138}_{82}$Ba shows at the Bass-barrier [60] a 2n-channel. The ratio of cross sections is a factor of 50 in favor of the $N = 82$ cluster-driven system.

shorter than for spherical nuclei of the same mass. A reduction in R/R_0 of less than 1 fm is indicated in Fig. 11. Compared to the total distance to be passed in the amalgamation stage this shortening is small. For deformed collision partners fusion

hindrance sets in already at $x = 0.68$, and complete fusion was until now never observed beyond $x = 0.79$, neither in the case of Pd or Nd, nor for actinide targets. The side collisions are the 'hugging collisions' discussed by A. Iwamoto and P. Möller [83]. Hugging is fine, but the couple warms up.

Finally, a systematic experimental study in support of SHE-synthesis for actinide-based reactions is missing. It was started using ^{232}Th-targets by A. Yeremin et al. [52] for projectiles up to ^{31}P ($x \leqslant 0.77$), but today it could be pushed to the limit $x = 0.81$ with ^{40}Ar-projectiles producing the known ^{267}Hs. Excitation functions for lower x-values using ^{22}Ne- and ^{26}Mg-projectiles peaking at 5n- and 6n-channels should be reanalyzed or remeasured in view of the nuclear structure of the deformed ^{232}Th and its supposed preference for side-collisions. With projectiles $Z = 8$–18 the whole range of the 'Coulomb Falls' ($x = 0.68$–0.81) could be covered for ^{232}Th targets, and these reactions could be used as a standard for all actinide-based reactions aiming beyond $Z = 108$.

4.3. Nuclear structure in the dynamics of the amalgamation stage

Nuclear structure is of great importance at low excitation energies in the rearrangements of nucleons during the amalgamation stage of fusion, though also this stage is ruled by the effective fissility, the macroscopic scaling parameter proportional to Z. The distance ΔR between the close-approach and the compound stage is the most important parameter for the passage. Into ΔR nuclear structure enters via the compound stage, as spherical nuclei are positioned in their ground-state at $R/R_0 = 0.75$, whereas the ground state of deformed nuclei is positioned at $R/R_0 = 0.85$. ΔR for reactions aiming at deformed SHE is shorter by 0.8 fm. The nuclear structure of deformed nuclei in the close-approach stage was discussed in the previous section. It was shown that the reduced distance in side-collisions suppresses the 2 lowest xn-channels, and makes fusion possible at higher excitation energies and smaller values of ΔR. The third parameter of importance in the amalgamation stage is the excitation energy of the configuration relative to the ground-state of the SHE. The level density of the system and the number of level-crossings shifting energy between the levels during the interpenetration of the collision partners is strongly nuclear structure dependant.

At low excitation energies in large nuclear rearrangement processes the structure of nuclear-subsystems was shown to be decisive, e.g., the asymmetric mass distribution in fission is determined to a large part by the clusters $N = 82$ and $Z = 50$ [84]. Also in fusion the use of $N = 82$-nuclei, as ^{138}Ba and ^{136}Xe combined with nuclei close to $N = 50$, as ^{82}Se and ^{86}Kr gives a surprise. Finally, strong nuclear structure is present in the doubly magic nucleus $^{208}_{126}\mathrm{Pb}_{82}$. It is this structure to which we owe the discovery of deformed SHE.

Fig. 16 presents the surprise. We compare the xn-channels and their cross sections for two reactions producing the same compound system ^{220}Th*, a condition not fulfilled in the former experiment with Kr/Xe [85], at nearly the same fissility: ^{70}Zn + ^{150}Nd ($x = 0.75$) from GSI [82] and ^{82}Se + ^{138}Ba ($x = 0.76$) from JAERI [86]. Lower x-values should show larger cross sections compared to larger x-values. However, we observe the contrary, a large difference between the systems, with larger cross sections for the Se/Ba-system. At the Bass-barrier 0.18 mb for Se/Ba compare to 4 μb for Zn/Nd giving a ratio of 45 for the cross sections. The strongest channels $\sigma(2\mathrm{n}) = 100$ μb for Se/Ba and $\sigma(4\mathrm{n}) = 0.2$ μb for Zn/Nd show a ratio of 50. The excitation functions for the system Zn/Nd were discussed already and corroborated the side-collisions hitting the deformed nuclei ^{150}Nd. The Se/Ba-reaction is open at the barrier, the 2n-channel dominates at the barrier, and the 1n-channel appears at the energy of 13 MeV, where 1n-channels should be expected. All higher channels down to the 6n-channel at the highest energy show cross sections decreasing regularly. This channel distribution observed at an x-value of 0.76 is characteristic for a system which is fully transmitted through a barrier at about 20 MeV. The on-set of fusion hindrance at $x = 0.72$ is delayed for ^{138}Ba by $\Delta x = 0.04$. We have met in Section 3 the system Se/Nd at $x = 0.79$ [63] with the deformed collision partner ^{150}Nd, and reported the disappearance of xn-channels at a nb-level. Now using the same projectile and the closed-shell nucleus ^{138}Ba a fully transmitted system with $\sigma = 0.18$ mb at the barrier is presented in Fig. 16. Within 4 atomic numbers σ-values drop by a factor larger than 17 going to the next higher element at constant projectile. In Fig. 7 a factor of 4 was given for ^{26}Mg as projectile, for targets with similar nuclear structure. The change of nuclear structure going from ^{138}Ba- to ^{150}Nd-targets causes the change from a factor 4 to a factor 17. What is demonstrated is pure action of nuclear structure in the amalgamation stage. The result is not a small correction, but a new quality, as unexpected as asymmetric fission had been more than 60 years ago.

My favorite experiment would be to follow the reactions between ^{138}Ba and the heavier partners: $^{86}_{50}$Kr, $^{88}_{50}$Sr, and Zr-isotopes. Is a free 1n-channel, as in ^{208}Pb-based reactions, the winning channel? The isotopes $^{224-x\mathrm{n}}$U, $^{226-x\mathrm{n}}$Pu, and $^{234-x\mathrm{n}}$Cm are well-suited for the EVR-α correlation technique. $^{139}_{82}$La is a second $^{209}_{126}$Bi and could reach the odd elements. The pair ^{138}Ba/^{139}La allows for most interesting collision systems. We learn on the lightest isotopes of elements above Th produced at good cross sections, and on cluster-based reaction mechanisms.

The ^{82}Se/^{138}Ba-reaction demonstrates as well, the universality of the mechanisms behind element synthesis, and enlightens the Pb/Bi-based element synthesis. Heavy clusters with shells at $N = 126$ and $N = 82$ start to show the decrease of cross sections in the 'Coulomb Falls' at a higher fissility, see Figs. 12 and 13. ^{138}Ba-induced reactions are delayed by $\Delta x = 0.04$, and as I pointed out in [87], Pb/Bi-induced reactions by $\Delta x = 0.07$. This is equivalent to a shift by 3 and 6 elements, respectively.

Not at $Z = 87$ and $Z = 96$, but at $Z = 90$ and $Z = 102$ starts the journey into the 'Coulomb Falls'. The systems ^{48}Ca/^{208}Pb ($x = 0.79$) and ^{26}Mg/^{232}Th ($x = 0.74$) are a similar couple as the one shown in Fig. 16, showing larger cross sections for the higher fissility. No-isotopes are reached, but slightly different compound nuclei ^{256}No* and ^{258}No* were formed. Ca/Pb populates (1n–3n)-channels [54] and Mg/Th (4n–6n)-channels [52], and there is no overlap of the populated channels. Comparing the channels at the barriers $\sigma(2n) = 3.4$ μb at $E^* = 20$ MeV for Ca/Pb, and $\sigma(4n) = 6$ nb at $E^* = 40$ MeV for Mg/Th, we obtain a ratio of 570 for the cross sections. The strongest channels $\sigma(3n)$ and $\sigma(5n)$ show a ratio of 380. The ratios for Ca/Pb–Mg/Th versus Se/Ba–Zn/Nd are larger by a factor of 10, maybe partly as we compare for the first couple different channels, maybe as there is a difference in shell-strength between ^{208}Pb and ^{138}Ba. The ratios $\sigma(2n)/\sigma(1n) = 13$ are equal for Ca/Pb and Se/Ba showing clearly that both systems are open at their barriers.

Comparing the strongest channels for the deformed nuclei ^{150}Nd and ^{232}Th we find a shift from 4n to 5n channels in correspondence to a difference of 10 MeV in the energies at the Bass-barrier. Not the deformed nuclei are surprising. The astonishment goes with the closed-shell collision partners, which both demonstrate the same behavior. Open channels are observed, where the fissility scaling already predicts large reductions of cross sections. Aiming at close-lying compound nuclei in each of the couples the geometrical distance ΔR in each of them is about equal, neglecting the small advantage of the warming up hugging collision systems. What is different are the excitation energies arriving at the compound state. For the strongest channel observed it is larger than 40 MeV for th ^{232}Th-induced reaction and less than 20 MeV for the ^{208}Pb-induced reaction. Beyond 40 MeV nuclear structure is lost in large scale rearrangement processes, e.g., asymmetric fission disappears. Below 20 MeV is the domain of nuclear structure dominated rearrangements in fission. Experiments show the existence of spherical, close shell clusters in the earliest stages accessible to measurements on fission fragments in low-energy, cold fission processes [84]. In the two-center level diagrams calculated by P. Möller et al. [88], gaps are found in the single particle energies for ^{86}Kr/^{136}Xe ($N = 50 + 82$) and ^{48}Ca/^{208}Pb ($N = 28 + 126$). In the level diagrams, the cluster (closed-shell) configurations are maintained until the deformation is reduced to $R/R_0 = 1.20$. In the final stage for $R/R_0 < 1.20$ the gaps in the level diagrams have disappeared. Dissipative dynamics with level crossings will act in the small range until the fission barrier of the deformed final product is reached at $R/R_0 = 1.05$. As the Möller-diagrams and the cold fission studies indicate, the heavy cluster configurations seem to survive far into the amalgamation stage of fusion, see Fig. 11.

The maximal cross sections for the cluster-based reactions in fusion are observed for 1n- and 2n-channels in the excitation energy range 10–15 MeV, that is at temperatures of the intermediate systems of $T = 0.7 - -0.9$ MeV, well below the limit of $T = 1.5$ MeV where shell corrections disappear. The translational velocities of the collision partners in this late stage of fusion are small and the excitation energy is restricted; both these conditions reduce dissipation. The underlying cluster may be excited but not destroyed. Nucleons out of shells carry most of the excitation energy and the clusters only a minor part. The available excitation energy allows the nucleons of the light partner to rearrange and to occupy the empty orbits outside the cluster core and finally to achieve transmutation into an excited state of the nascent heavy nucleus. Amalgamation and transmutation, words out of the baggage of alchemists, indicate that we do not understand in detail how things really happen either in asymmetric fission or in cluster-based fusion. We know they do happen, and we are patient to learn why they do.

A configuration close to the deformation of the protecting fission barrier of the final nucleus at an excitation of an 1n-channel would be protected against immediate reseparation having emitted the neutron and having cooled down to a state below the fission barrier. Since the macroscopic forces ruled by the high effective fissility are repulsive in all stages of the collision, the system stays in the favorable position $R/R_0 = 0.85$–1.05 only for a short time compared to the emission time of an 1n-channel neutron. The Γ_n/Γ_f-value of such a precompound-emission process will be very small. It is this large reduction of the survival probability for the precompound 1n-channel which destroys the large advantage compared to a deexcitation by 4n and 5n-channels from actinide-based reactions. Actually, the observed cross sections (Fig. 7) tell us that the difference using the Pb/Bi-method or the actinide-method to produce SHE is smaller than a factor of 10 in favour of the cluster-based reaction. The scenario of precompound n-emission would be a reaction never reaching the compound stage, a sort of one-step, direct reaction. Support of such a scenario comes from the lack of observation of the capture channel in Pb/Bi-based reactions. Deexcitation by high energy γ-rays takes longer than the emission of a single fast neutron, and γ-emission has no chance to compete in the short time interval of closest approach.

The proposed scenario is a one-step rearrangement process restricted to low energy fusion reactions. It is not competitive for the emission of several neutrons at higher excitation energies. The multistep deexcitation scenario with an equilibrated compound system stays valid for actinide-based reactions and all other reactions discussed. At very high fissilities ($x = 0.80$) precompound multiple α-emission may announce incomplete fusion reactions, which populate again compound systems at lower atomic numbers cooling down by multistep neutron emission.

The one-step, one-neutron scenario is conditioned by a heavy cluster avoiding dissipative heating over long distances in the amalgamation stage, as indicated in Fig. 11. The heavy cluster stays cool. This is an achievement of nuclear structure in reaction dynamics. It complements the manifestation of nuclear structure stabilizing the ground-state of SHE. The 'Coulomb Falls' = increasing fissilities = disappearing pockets impose element synthesis to be an intrinsically self-terminated process. Nuclear structure is a consolation to this hard message. It gives to SHE – to the aim of our game, ground-state protection

against spontaneous fission – the reason for their existence. It gives to fusion – to our tool, the shell-stabilized clusters keeping the process cool – the chance to reach $Z = 112$, an element 12 atomic numbers above $Z = 100$, the estimated end of the Table of Elements at a time when nuclear structure in reaction dynamics was still ignored.

5. Prospects, what has to be done

5.1. Dreams make turn the wheel

The task of those who follow my conclusions, is to consolidate the message by further experiments accepting the close end of element synthesis at $Z = 112 + \varepsilon$, with ε equal to 1 or 2 in complete fusion reactions. I am aware the number of non-believers will be a majority. The dreams of a second island of elements behind U to be put to use, is old, and gave one of the strong reasons to start building GSI in 1969. 30 years later the dream has slightly changed. Spherical SHE up to $^{298}120$ became the new philosopher's stone helping to raise new funds. In 2002 we count five laboratories well-equipped with modern accelerators and recoil separators ready for hunting new elements. Whatever the newcomers will try and do, finally, if well done, they all will help to consolidate our scientific field. There is one scientific truth, even if found by trial and error. Hopefully, now open still controversial problems will have been settled in a not too far future by the new common effort.

Once more [51,89], I have to comment shortly on an open problem: the work driven by Yu. Oganessian [90–93] which claims to have made, beyond the limits of the 'Coulomb Falls' at $x = 0.84$–0.88 superheavy isotopes of the elements $Z = 110, 112, 114$, and 116 by complete fusion of ^{48}Ca and actinides. Beyond this limit we find as well the cluster-driven reactions which I have discussed extensively. Compared to ^{208}Pb the shell-corrections of ^{48}Ca are weak and we have no experimental proof that its extra-neutrons foster fusion. Actinides have deformed nuclei, and until now nobody succeeded to induce complete fusion using deformed nuclei at $x > 0.79$. ^{48}Ca and actinide nuclei should not fuse anymore. From lighter projectiles (^{22}Ne, ^{26}Mg, ^{27}Al) we know that climbing to higher elements by 6 atomic numbers using the targets between ^{232}Th and ^{248}Cm is paid by a decrease in cross sections by more than a factor 10^3. The cross sections reported are nearly constant. Why should ^{48}Ca break this decrease of cross sections governed by increasing Coulomb forces? To make elements 110 and 116 with about the same cross section should be impossible. The work presented does not concern the xn-channels of complete fusion. Whatever else it may concern, the game ^{48}Ca/^{248}Cm is certainly interesting and worthwhile to be continued. But, it will not give elements beyond the 'Coulomb Falls'. N-rich isotopes beyond reach of xn-channels of elements $Z \leqslant 110$ in the chains around $(N - Z) = 60$ produced by incomplete fusion are one option in the open outcome of multinucleon exchange reactions on the 1 pb-level. Chemists searching for the reported longer lived sf-activities may identify the emitters as isotopes of Sg and Rf. Not verifying the physics experiments, they may help physicists to correctly interpret the facts, as was once done in 1938 by the chemists O. Hahn and F. Straßmann [94].

5.2. Reaction studies

The fusion reaction studies to be done should follow systematics, should be of high experimental standards, equipped with sufficient beamtime, and carried out over the years with patience. I recall the discussion on nuclear structure in the previous section, and the proposals therein as to what could be done. The studies at the limits in the 'Coulomb Falls' are of special importance. They need most patience and beamtime. They may open new methods in isotope production, but hopefully will lead to new reaction mechanisms, the begin of all further progress. Once noted that beyond the 'Coulomb Falls' we enter, with incomplete fusion reactions, the vast region of multiple break-up reactions, that is the second half of the reactions presented in Fig. 12, new prospects also of element synthesis may be discovered.

Nuclear structure may have new surprises in reactions kept at a temperature level where nuclear structure has a chance to survive. Binary and ternary reactions up to the heaviest collision partners may give SHE-clusters a chance to survive the collision. We may speculate that the collision system $^{238}_{146}$U/$^{248}_{152}$Cm at energies close to its Coulomb barrier kept at a small excitation energy, and having reached $R/R_0 \approx 1.3$ may be driven to transmute into the cluster $^{298}_{178}120$ and $^{188}_{120}$Er, a heavy version of the standard I channel [95] in asymmetric fission. The system ^{186}W/^{248}Cm may disintegrate into two clusters ($^{304}_{184}120 + {}^{130}_{80}$Sn), a heavy version of symmetric fission of ^{258}Fm into a pair of Sn-clusters [96,97]. As we know [98], the heaviest collision systems produce mainly hot reaction products in deep-inelastic reactions, but at an 0.1 pb-level at low excitation energies we may meet nuclear structure supported dynamics, as we have encountered on our way down the 'Coulomb Falls' in fusion. There may still be something hidden in the virgin forest of nuclear reactions beyond complete fusion. Certainly, multi-nucleon transfer reactions ($R/R_0 > 1.6$), deep-inelastic reactions ($R/R_0 = 1.4$–1.6), quasi-fission ($R/R_0 = 1.2$–1.4) and incomplete fusion ($R/R_0 = 1.0$–1.2) may give new isotopes in the transactinide region. Less certain, as speculated, cluster driven dynamics in any cold break-up environment ($E^* < 30$ MeV) may produce SHE-residues.

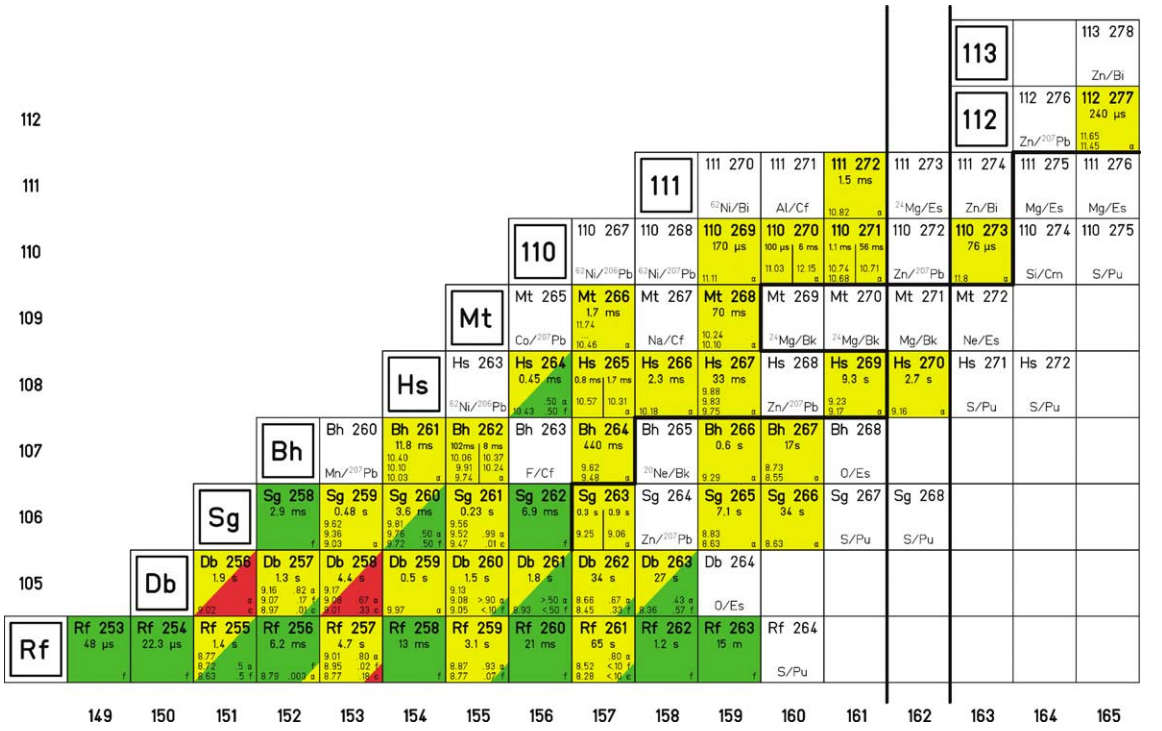

Fig. 17. The isotopes of elements 104 to 113 accessible above the σ-level of 0.1 pb. The known isotopes are given. Green: spontaneous fission, yellow: α-decay. The recommended collision systems for the elements and isotopes not yet synthesized are indicated in the blank boxes.

5.3. New elements and isotopes in the 'Coulomb Falls' of fusion

Accepting the dramatic loss of fusion cross sections in the 'Coulomb Falls', we can exploit cross sections down to the limit set be the experimental methods, $\sigma > 0.1$ pb. This is the restriction for our search for new elements and isotopes. The highest atomic numbers to be reached with a deformed actinide nucleus and a cluster-driven reaction using Bi are 111 and 113, respectively. As shown, there remains a minor advantage for the latter type of reactions. Fig. 17 amplifies the small triangle indicated in Fig. 2 of about 50 deformed isotopes of SHE, and shows a chart of nuclides of the 46 known transactinide isotopes in 2002, and the still unknown isotopes with collision partners proposed for their production. Out of the isotopes shown only about half have been synthesized to date. Of the isotopes still to be made about 2/3 need actinide-based reactions.

The heaviest actinide isotopes ^{254}Es, ^{249}Cf, ^{249}Bk, ^{248}Cm, and ^{244}Pu available as targets combined with the most n-rich projectiles between ^{18}O and ^{36}S promise the best production rates for actinide-based reactions. The highest element possibly accessible is element 111 to be produced with ^{249}Cf or ^{254}Es-targets ($x = 0.80-0.81$). $N = 166$ is reached with the isotope ^{276}110 by ^{36}S on ^{244}Pu. This reaction gives also the heaviest isotopes of Hs, Sg, and Rf. ^{268}Sg will be a chain member on the $N = 162$-shell. This shell should be accessible directly from Hs to $Z = 111$. The long-lived isotopes at $N = 160-162$ have opened the field for chemistry experiments up to Mt. The chemistry of Hs was investigated and the new isotope ^{270}Hs in the center of the deformed SHE was discovered [49].

The Pb/Bi-based reactions need, besides ^{208}Pb and ^{209}Bi, the targets ^{206,207}Pb to be combined with the n-rich projectiles ^{62,64}Ni and ^{70}Zn. The chances to discover one day element 113 in the reaction ^{70}Zn/^{209}Bi are not bad. Another challenge is to find more e–e isotopes of elements 110 and 112 populating the chains $N-Z = 48$–52. The $N-Z = 52$-chain passes the $N = 162$-shell. To find all the missing α-bridges at ^{262}Sg and ^{258,260}Rf requires a special effort. The α-energies connect the region of deformed SHE around ^{270}Hs to the masses of known isotopes. There is no better way to fix a closed shell than by the measurement of mass excesses. The existence of deformed barrel-like ($\beta_4 < 0$) SHE was one of the most rewarding discoveries for experiments and theory, and the measured shell strength would be a stringent test of microscopic theory.

In-beam γ-spectroscopy of transactinide isotopes is within reach. The isotope ^{254}No is produced with a good cross section in ^{48}Ca/^{208}Pb. Two experiments combining recoil spectrometers and large γ-arrays succeeded in observing the ground-state band of ^{254}No up to spins $I = 14$ [99] and $I = 16$ [100]. ^{254}No is found to be good rotor, with a β_2-value of 0.27 ± 0.02. Its first 2^+ state at 44 keV is in good agreement with a predicted value of 42.4 keV [101]. Up to $I = 16$ and $E^* = 6.2$ MeV the nucleus ^{254}No is still not destroyed by fission. The production of transactinides certainly has smaller cross sections, but the new

technique is still full of possible improvements. It will open the field of nuclear structure studies of the heaviest elements, and we will learn how high spin values and excitation energies reduce the fission barrier and increase the Γ_f values.

6. Conclusions

In this article you will miss formulae and mathematics. I restricted myself to describing observations, to explaining rather extensively the figures, which are the backbone of the text, and to selecting what I think should be transmitted to the reader. I presented in the three main sections the three great discoveries in the field, in which I had the good fortune to be involved.

There is no island of SHE, but one continent of the world of nuclei. A way was opened along $N-Z = 52\pm2$ to shell-stabilized elements, the deformed SHE [11–14]. We made, using spherical ^{208}Pb, deformed SHE up to element 112, the contrary of what was recommended to be done, to use deformed actinide nuclei in order to produce spherical SHE.

Producing EVR by fusion of lighter elements we learnt that fusion is limited to about half of the possible combinations of available collision partners. Together with parallel work on binary reactions the 'Coulomb Falls' was experimentally established, an idea which was propagated and developed before experiments started [68].

The fusion reactions using Pb/Bi-nuclei gave at very low excitation energies of about 13 MeV in 1n-channels new elements at fissilities where other collision systems refused to fuse at all [50,51]. The action of the shell-stabilized clusters in the dynamics was established in fusion [87], as was done before in fission [96].

Acknowledgement

All experiments I was involved were done in groups, and here my gratitude goes to the SHIP-group, which I managed to bring together along time ago. We worked together over more than 20 years. Thanks to all of them, especially to G. Münzenberg, S. Hofmann, and F.P. Heßberger for new elements, and to K.-H. Schmidt and W. Reisdorf for reaction studies. It was, for me, a great time; thank you all once more.

References

[1] P. Armbruster, Annu. Rev. Nucl. Part. Sci. 35 (1985) 135.
[2] Y.T. Oganessian, A.S. Iljinov, A.G. Demin, S.P. Tretyakova, Nucl. Phys. A 239 (1975) 353.
[3] S. Hofmann, et al., Z. Phys. A 354 (1996) 229.
[4] G. Münzenberg, et al., Z. Phys. A 300 (1981) 107.
[5] G. Münzenberg, et al., Z. Phys. A 309 (1982) 89.
[6] G. Münzenberg, Z. Phys. A 317 (1984) 235.
[7] A. Ghiorso, et al., Phys. Rev. Lett. 33 (1974) 1490.
[8] H. Meldner, Ark. Fys. 36 (1967) 593.
[9] A. Sobiczewski, F.A. Gareev, B.N. Kalinkin, Phys. Lett. 22 (1966) 500.
[10] A. Sobiczewski, Nobel Symposium 27 Physics, Phys. Scripta A 10 (1974) 47–52.
[11] S. Cwiok, et al., Nucl. Phys. A 410 (1983) 254.
[12] A.G. Demin, S.P. Tretyakova, V.K. Utyonkov, I.V. Shirokovsky, Z. Phys. A 315 (1984) 197.
[13] G. Münzenberg, et al., Z. Phys. A 315 (1984) 145.
[14] P.J. Armbruster, "Enrico Fermi" School, Varenna 1984, Course 91, North-Holland, Amsterdam, 1986, p. 222.
[15] S. Hofmann, et al., Z. Phys. A 350 (1995) 277.
[16] S. Hofmann, et al., Z. Phys. A 350 (1995) 281.
[17] G. Leander, et al., in: O. Klepper (Ed.), Proc. Int. Conf. AMCO 7, TH-Darmstadt, 1984, p. 466.
[18] K. Böning, Z. Patyk, A. Sobiczewski, S. Cwiok, Z. Phys. A 325 (1986) 479.
[19] A. Sobiczewski, Z. Patyk, S. Cwiok, Phys. Lett. B 186 (1987) 6.
[20] K.-H. Schmidt, et al., in: Proc. Int. Conf. Phys. Chem. Fission, Jülich, 1979, Vol. 1, IAEA, Vienna, 1980, p. 409.
[21] S. Polikanov, et al., Soviet Phys. JETP 15 (1962) 1016.
[22] F.P. Hessberger, et al., Z. Phys. A 321 (1985) 317.
[23] G. Münzenberg, et al., Z. Phys. A 322 (1985) 277.
[24] G. Münzenberg, et al., Z. Phys. A 324 (1986) 489.
[25] P. Möller, J.R. Nix, At. Data Nucl. Data Tables 26 (1981) 165.
[26] W.J. Swiatecki, Phys. Rev. 100 (1955) 937.
[27] P. Armbruster, et al., in: O. Klepper (Ed.), Proc. Int. Conf. AMCO 7, TH-Darmstadt, 1984, p. 284.
[28] Z. Patyk, A. Sobiczewski, P. Armbruster, K.-H. Schmidt, Nucl. Phys. A 491 (1989) 267.
[29] P. Möller, J.R. Nix, in: Proc. Int. Conf. Phys. Chem. Fission, Rochester, 1973, Vol. 1, IAEA, Vienna, 1974, p. 103.

[30] R. Smolanczuk, J. Skalski, A. Sobiczewski, Phys. Rev. C 52 (1995) 1871.
[31] R. Smolanczuk, Phys. Rev. C 56 (1997) 812.
[32] K.-H. Schmidt, D. Vermeulen, in: J.A. Nolen, W. Benenson (Eds.), AMCO-6, Plenum, New York, 1980, p. 119.
[33] N. Zeldes, T.S. Dumitrescu, H.S. Köhler, Nucl. Phys. A 399 (1983) 11.
[34] T.H.R. Skyrme, Nucl. Phys. 9 (1959) 635.
[35] D. Vautherin, D. Brink, Phys. Lett. B 32 (1970) 149.
[36] D. Vautherin, M. Vénéroni, D.M. Brink, Phys. Lett. B 33 (1970) 381.
[37] P. Quentin, H. Flocard, Annu. Rev. Nucl. Part. Sci. 28 (1978) 523.
[38] F. Tondeur, Z. Phys. A 297 (1980) 61.
[39] J. Dechargé, D. Gogny, Phys. Rev. C 21 (1980) 1568.
[40] H.P. Dürr, Phys. Rev. 103 (1956) 469.
[41] P.G. Reinhard, Rep. Prog. Phys. 52 (1989) 439.
[42] S. Cwiok, et al., Nucl. Phys. A 611 (1996) 211.
[43] K. Rutz, et al., Phys. Rev. C 56 (1997) 238.
[44] M. Bender, et al., Phys. Rev. C 60 (1999) 034304.
[45] P. Ring, Prog. Part. Nucl. Phys. 37 (1996) 193.
[46] J. Dechargé, J.F. Berger, K. Dietrich, M.S. Weiss, Phys. Lett. B 451 (1999) 275.
[47] M. Bender, et al., Phys. Lett. B 515 (2001) 42.
[48] P. Bonche, private communication, July 2002.
[49] C.E. Düllmann, et al., Nature 418 (2002) 859.
[50] S. Hofmann, G. Münzenberg, Rev. Mod. Phys. 72 (2000) 733.
[51] P. Armbruster, Ann. Rev. Nucl. Part. Sci. 50 (2000) 411.
[52] A.V. Yeremin, et al., NIM B 126 (1997) 329.
[53] A.N. Andreyev, et al., Z. Phys. A 345 (1993) 389.
[54] H.W. Gäggeler, et al., Nucl. Phys. A 502 (1989) C561.
[55] K.-H. Schmidt, W. Morawek, Rep. Progr. Phys. 54 (1991) 949.
[56] J.G. Keller, et al., Nucl. Phys. A 452 (1986) 173.
[57] C.-C. Sahm, et al., Nucl. Phys. A 44 (1985) 316.
[58] B. Quint, et al., Z. Phys. A 346 (1993) 119.
[59] W. Morawek, et al., Z. Phys. A 341 (1991) 75.
[60] R. Bass, Lecture Notes in Phys., Vol. 117, Springer-Verlag, Heidelberg, 1980, p. 281.
[61] W. Reisdorf, Z. Phys. A 300 (1981) 227.
[62] D. Vermeulen, et al., Z. Phys. A 318 (1984) 157.
[63] K. Nishio, JAERI-Rev. 2001-030 (2001) 37.
[64] K. Nishio, et al., Phys. Rev. C 62 (2000) 014602;
K. Nishio, et al., Phys. Rev. C 63 (2001) 044610.
[65] V.Yu. Denisov, W. Nörenberg, Eur. Phys. J. A 15 (2002) 375.
[66] J. Blocki, H. Feldmayer, W.J. Swiatecki, Nucl. Phys. A 459 (1986) 145.
[67] R. Bass, Nucl. Phys. A 231 (1974) 141.
[68] W.J. Swiatecki, Phys. Scripta 24 (1981) 113.
[69] J. Töke, Nucl. Phys. A 440 (1985) 327.
[70] W.Q. Shen, et al., Phys. Rev. C 36 (1987) 115.
[71] W. Reisdorf, et al., Z. Phys. A 342 (1992) 411.
[72] Y.A. Lazarev, et al., Phys. Rev. Lett. 75 (1995) 1903.
[73] S. Hofmann, F.P. Hessberger, private communication, 2001.
[74] W. Reisdorf, M. Schädel, Z. Phys. A 343 (1992) 47.
[75] S. Bjornholm, A. Bohr, B.R. Mottelson, in: Proc. Int. Conf. Phys. Chem. Fission, Rochester, Vol. 1, IAEA, Vienna, 1974, p. 367.
[76] A. Junghans, et al., Nucl. Phys. A 629 (1998) 635.
[77] A.V. Ignatyuk, et al., Soviet J. Nucl. Phys. 21 (1975) 612.
[78] A. Heinz, et al., Nucl. Phys. A 713 (2003) 3.
[79] P. Cagarda et al., GSI Scientific Rep. 2001, GSI 2002-1, 2002, ISSN 0174-0814, p. 15.
[80] D.J. Hinde, et al., Phys. Rev. C 53 (1996) 1290.
[81] S. Mitsuoka, et al., Phys. Rev. C 65 (2002) 054608.
[82] Ch. Stodel, Etude expérimentale de l'influence de la structure des partenaires dans la fusion de systèmes presque symétriques, Thesis, Univ. Caen, 1998.
[83] A. Iwamoto, et al., Nucl. Phys. A 596 (1996) 329.
[84] P. Armbruster, Rep. Progr. Phys. 62 (1999) 465.
[85] Yu. Oganessian et al., Ann. Rep. 1995/96 JINR-FLNR Dubna (1997) p. 62.
[86] K. Satou, et al., Phys. Rev. C 65 (2002) 054602.
[87] P.J. Armbruster, "Enrico Fermi" School, Varenna 1987, Course 103, North-Holland, Amsterdam, 1989, p. 282.
[88] P. Möller, et al., Z. Phys. A 359 (1997) 251.
[89] P.J. Armbruster, Eur. Phys. J. A 7 (2000) 23.

[90] Y.T. Oganessian, et al., Phys. Rev. Lett. 83 (1999) 3154.
[91] Y.T. Oganessian, et al., Nature 400 (1999) 242.
[92] Yu. Oganessian, et al., Phys. Rev. C 62 (2000) 041604 (R).
[93] Yu. Oganessian, et al., Phys. Rev. C 63 (2001) 011301 (R).
[94] O. Hahn, F. Strassmann, Naturwiss. 27 (1939) 11.
[95] U. Brosa, et al., Z. Naturforsch. 41 (1986) 1341.
[96] H. Faissner, K. Wildermuth, Nucl. Phys. 58 (1964) 177.
[97] D.C. Hoffman, et al., Phys. Rev. C 21 (1980) 972.
[98] M. Schädel, et al., Phys. Rev. Lett. 48 (1982) 852.
[99] P. Reiter, et al., Phys. Rev. Lett. 82 (1999) 809.
[100] M. Leino, et al., Eur. Phys. J. A 6 (1999) 63.
[101] I. Muntian, Z. Patyk, A. Sobiczewski, Phys. Rev. C 60 (1999) 041302.